ENERGY LEVELS AND DECAY SCHEME OF LANTHANUM-135

David Barzilay

A THESIS

in

The Department

of

Physics

Presented in Partial Fulfillment of the Requirements for

the Degree of Master of Science at

Sir George Williams University

Montreal, Canada

March, 1972

TABLE OF CONTENT

ACKNOWLEDGEMENTS

The author wishes to thank Dr. N. Eddy for his interest, guidance and constant encouragement during the course of the research.

In addition, the author wishes to thank Mr. S. Muszynski for his assistance in the negotiations for the use of the McGill cyclotron and subsequent helpful descussions, Dr. Misra for allowing the use of his X-ray detector.

Thanks are also extended to Mr. L. Barbopoulos and Mr. J. Clark for their helpful discussions.

A B S T R A C T

ENERGY LEVELS and DECAY SCHEME of LANTHANUM-135

The gamma rays of lanthanum-135 following the (p, 4n) reaction on barium-138 were studied with a 35cc lithium drifted germanium, Ge(Li), detector and 3" x 3" sodium iodide, NaI (Tl), detector. A total of ten gamma rays with energies 221.8, 269,5, 366.5, 374.5, 481.4, 588.2, 634.0, 654.6, 856.0 and 875.4 keV were observed (errors of which were less than 0.5 keV) and attributed to La^{135}, Gamma-gamma coincidence measurements have led to the most probable decay scheme. X-ray-gamma ray coincidence experiments were also performed, giving further verification of the identity of the gamma-rays.

LIST OF DIAGRAMS

CHAPTER I

INTRODUCTION

Lanthanum - 135, (La^{135}), decays by electron capture [1] with a half life of 19.8 ± 0.2 hours. Other half life measurements as performed by S. Morinbu et al[2] gives a value of 19.4 ± 0.1 hours. Previous attempts of devising a decay scheme of La^{135} resulted in several inconsistencies as regards to decay scheme systematics. It was not until studies by H.A. Grench [3] and S. Morinbu et al[2] that more reliable results for energy levels and more consistent decay schemes were found. H.A. Grench [3] studied the gamma rays from the (α,2n) reaction on Cesium - 133, (Cs^{133}) and reported energies corresponding to the excitation of four energy states in the residual nucleus, Ba^{135}, including an isomeric state. The energy values they found were 218, 481, 587 and 865 keV and 268 keV for the isomeric state. In addition, they reported gamma rays with energies of 108, 256, 367, 375 and 640 keV.

S. Morinbu et al[2] observed new gamma ray transitions of 373, 633, 655 and 852 keV energies. The 268 keV transition they found to be absent. They produced the La^{135} activity via the (p,4n) reaction on Barium - 138, Ba^{138}. In addition to their gamma and beta spectroscopic measurements, they also performed measurements of internal conversion electrons and logft values, from which they were able to assign spins and parities to the energy levels of Ba^{135}. Their proposed decay scheme is shown in Figure A

In the work presented here, gamma and X-ray measurements were performed on the activated sample of La^{135}, produced by the Ba^{138}

(p, 4n) La^{135} reaction. For this purpose, three detectors were used. These were: a lithium drifted germanium detector, a thallium doped sodium iodide detector and a lithium drifted silicon detector. Previous investigations involved only the use of scintillation detectors such as the sodium iodide. The first and third detectors quoted above are solid state detectors and allow for more refined and accurate measurements on the gamma rays, due principally to a much better resolution. This improvement of resolution is extremely important since it allows for the possibility of observing gamma rays which had previously not been reported and provides more precise assignments of the energy values associated with the gamma rays. It was with this purpose that this work was undertaken.

The detectors, their mode of operations and relative merits of use are discussed in Chapter II, Also in this chapter, the electronic equipment used throughout the investigations are discussed.

In Chapter III the preparation of the source and half life measurements performed on it along with the energy calibration procedure are discussed. In the final sections of this chapter, all the results obtained from the "singles" spectra of the gamma rays and from gamma-gamma and X-ray-gamma coincidence measurements are tabulated and the respective spectra shown.

A discussion of the relative merits of gamma ray spectrocopy for the study of energy levels and construction of decay schemes, and a simplified theory of beta decay which leads to the selection rules of the energy transitions along with the selection rules for gamma ray transitions is given in Chapter IV. Finally in this chapter, the

analysis used for the construction of the decay scheme of La^{135} based on the results obtained is given along with the final proposed decay scheme and the conclusions drawn.

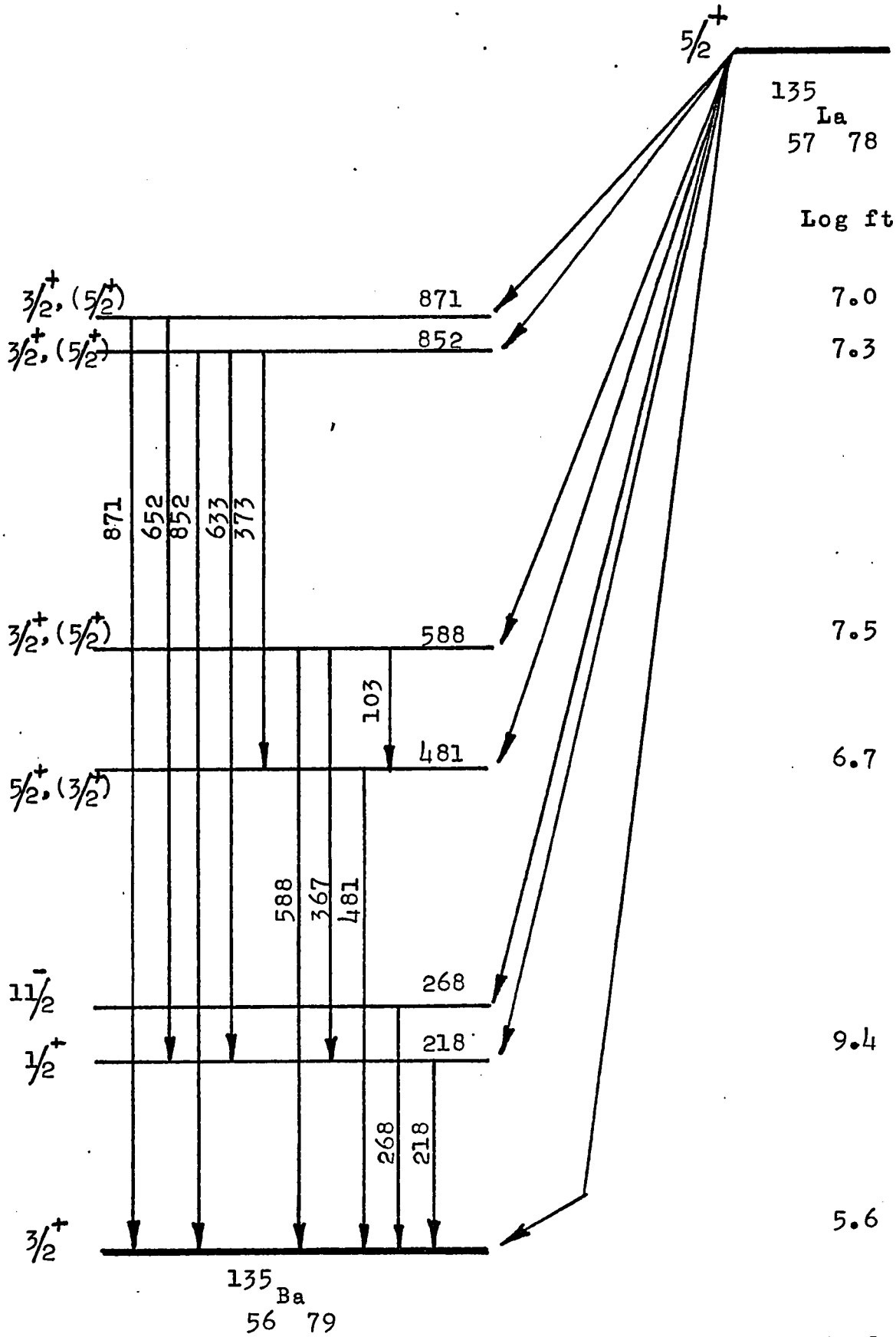

Figure A. Decay scheme proposed by S. Morinbu et al.
(All energies in keV)

CHAPTER II

DETECTORS AND ASSOCIATED ELECTRONICS.

2.1 The Lithium Drifted Germanium Detector.

In the past few years, great efforts have been directed towards the development and improvement of semiconductor radiation detectors, (Goulding[4]). In a general sense one can think of this type of detector as a solid state ionization chamber, having two basic advantages over a gas filled ionization chamber:

a) The energy required for the creation of an electron-ion pair is 3eV (as compared to approximately 30eV in a gas) so that stronger signals and better statistics can be achieved.

b) The stopping power is approximately 10^3 times that of a gas filled device (since the detector material is so much denser), and thus it becomes possible to stop, in the detector, particles with energies typical of nuclear interactions. Consequently a very large number of electron-ion pairs is formed leading to a very good energy resolution.

The germanium, lithium drifted, Ge(Li), detector used here was supplied by the Nuclear Diodes Corporation of Chicago (Model LGTC 4.0x). The detector is mounted on a cold finger of a liquid nitrogen cryostat in a right angle geometry. The nominal volume being 35 cubic centimeters, the cross-sectional shape is a true coaxial one with an area of 10.3 square centimeters, the active area has a length of 33 mm. The whole detector is vacuum encapsulated in an aluminium can. The intrinsic side of the detector is facing forward and is a few millimeters from the cap.

This detector has a large photoelectric absorption cross-section and hence is very well suited for gamma ray studies. Because of the small amount of energy required to liberate an electron-ion pair in the detector, it must be operated at low temperatures (normally at liquid nitrogen temperature, 77^{o}K) in order to minimize the thermal noise in the detector.

The performance of the entire detection system depends ultimately on how well the detector performs. The detector is a p-i-n junction device manufactured by drifting lithium ions through p type Germanium under a strong electric field and carefully controlled conditions. This process precisely compensates for the excess p type impurities originally present in the germanium, thus producing a region of high resistivity (intrinsic region) material. The resulting configuration is a compensated region (sensitive region) with p-type, undrifted, material on one end of a cylindrical surface and n-type on the other end.

Fast and efficient collection of electron-hole pairs is to be desired in the detector. This is influenced both by the quality of the intrinsic region and by the field strength applied. The field strength should be high enough so that the fraction of the charged pairs collected is independent of the energy of the ionization radiation, but not high enough to cause electrical breakdown. The quality of the intrinsic region is manifested in the number of centers through its volume that neither trap ion pairs nor inhibit their collection.

General noise contributions from the detector, which arise from a number of sources, result in increased electronic noise in the system, and this increase is essentially independent of the energy of the gamma rays to be detected. A common source of detector noise is the amount of leakage current from one junction to the other through the surface states, (the chemical state of all the detector surfaces formed during the final chemical step prior to the actual encapsulation of the detector is referred to as the surface state), of the intrinsic region. Surface state leakage current should remain less then 1nA. A minor source of noise sometimes encountered is that due to injection of carriers at the contact points where the bias voltage is applied to the detector. This is usually eliminated by cleaning or changing the contacts or by applying liquid metal to the surface of the detector at the point of contact.

When a gamma ray enters the detector, several processes compete. The gamma ray may pass through it without losing any of its energy; it may lose part of it via Compton scattering; or it may be absorbed completely by the photoelectric effect. The second type of event gives a continuous pulse height distribution, while the last type of event results in a well defined peak in the pulse height spectrum. The great advantage of the Ge(Li) detector, as mentioned previously, is the very much improved energy resolution that it offers. The resolution of the detector is defined by:

$$\text{Resolution} = \frac{\text{full width at half maximum}}{\text{energy}}$$

The basic limitation on the energy resolution of a Ge(Li) detector is the statistical fluctuation in the number of ion pairs created for a given energy. This limit involves the Fano factor. If one considers a gamma ray whose energy E is completely absorbed within the intrinsic region of the Ge(Li) detector, part of its energy goes into the formation of ion pairs and part of it goes into heating the lattice crystal structure (phonon or thermal energy). The Fano factor is defined as the ratio of the variance to the yield. The yield is the number of electron-hole pairs produced for a given amount of energy deposition E, while the variance, σ^2, is the mean square variation of the yield. If the number of electron volts required to produce an ion pair in germanium is given by ϵ, then the yield is,

$$y = E/\epsilon$$

and the Fano factor is,

$$F = \frac{\sigma^2}{E/\epsilon}$$

The division of energy between heating and ionization is essentially statistical. Without the competing process of heating, all the incident energy would result in ion pair production and there would be no statistical fluctuation, thus F = 0. If on the other hand, the probability of ion pair production is small, resulting in a very large ϵ, Poisson statistics would be expected to hold and the variance would equal the yield, thus F = 1. The evaluation of the full width at half maximum (F W H M) for each energy peak is discussed in Chapter III section 3.4. The resolution of the Ge(Li) detector as obtained from Nuclear Diodes has a F W H M of 2.9 keV. for the 1333 keV gamma ray of Cobalt-60

2.2 The Sodium Iodide and the X-Ray Detectors

Along with the Ge(Li) detector sodium iodide, thallium doped, detector, NaI(Tl) was extensively used. Its use in evaluating the absolute efficiencies of the Ge(Li) detector for different gamma ray energies will be discussed in section 2.4 of this chapter. In the subsequent coincidence measurements that were performed this detector was utilized to detect the "gated" gamma ray. This will be discussed later. Although its energy resolution is poorer than that of the Ge(Li) detector, it does however offer a higher efficiency which is important in coincidence work. This detector consists mainly of a luminescent crystal and a photomultiplier. When a photon enters such a crystal, NaI activated by thallium, and is absorbed by one or more of the atoms, a fast photoelectron is ejected. As it moves through the crystal, it ionizes and excites the atoms of the crystal along its path until its whole energy is transferred to the crystal. The event lasts for a short time interval of the order of 10^{-8} sec. The excited atoms radiate, emitting photons of visible light or ultra violet light. The crystal is placed in optical contact with the plane window of a photomultiplier, and the photocathode is mounted near the window. To improve the collection and transmission of light to the photocathode, the face of the crystal making contact with the photomultiplier is covered with a thin film of transparent oil. The remaining faces of the crystal are covered with material which scatters light back to the crystal, magnesium oxide is often used. The relative merits of using this detector will be discussed in Section 2.4 of this chapter.

The X-Ray detector used in this work was a silicon solid state detector lithium drifted, Si(Li), purchased from Simtec, model K-03S. The primary purpose of the use of this detector was to obtain the characteristic X-ray spectrum of the irradiated sample under investigation. In addition, it was used in conjunction with the Ge(Li) detector to perform X-ray - gamma ray coincidence measurements. These are discussed in the next chapter.

2.4 Efficiencies of Detectors.

Before the Ge(Li) detector may be of great use in gamma ray measurements, its photoelectric (or photopeak) efficiency for Gamma rays of different energies must be known. There are principally two ways of specifying efficiency:

$$\text{absolute efficiency} = \frac{\text{Total counts in the peak only, in time t}}{\text{Total disintegration of source, in time t}} \cdot \quad \text{(i)}$$

Efficiency relative to 3" x 3" NaI(Tl)

$$= \frac{\text{absolute efficiency of Ge(Li)}}{\text{absolute efficiency of NaI(Tl)}} \quad \text{(ii)}$$

one also defines intrinsic efficiency by

$$\text{intrinsic efficiency} = \frac{\text{absolute efficiency}}{\text{geometric efficiency}} \quad \text{(iii)}$$

The geometric efficiency is just the fractional solid angle and is equal to the detector area divided by $4\pi R^2$ with R being the source to detector distance for a point source. The three standard sources used in performing the necessary calculations were Co^{60}, Cs^{137} and Co^{57}.

Using equation (c) with known values of the intrinsic efficiencies the absolute efficiencies of the NaI(Tl) detector for different energies were calculated for our source-to-detector distances; then from equation (a), the total number of disintegrations of the respective sources, per second, were found. Making use of the Ge(Li) detector to obtain the total counts in the peaks and using equation (a) with the knowledge of the total disintegrations per second, previously found, the absolute efficiencies of the Ge(Li) detector for the different gamma ray energies were calculated. The values obtained for the absolute efficiencies are strong functions of the source to detector distance. These results are shown in Table 1 and the corresponding curves of absolute efficiency versus source to detector distance are displayed in Figures 1a, 1b and 1c.

Figures 1a, 1b and 1c

Calibration curves of absolute efficiencies versus source to detector distance for the Ge(Li) detector for energies of 1333, 662 and 122 KeV gamma rays respectively.

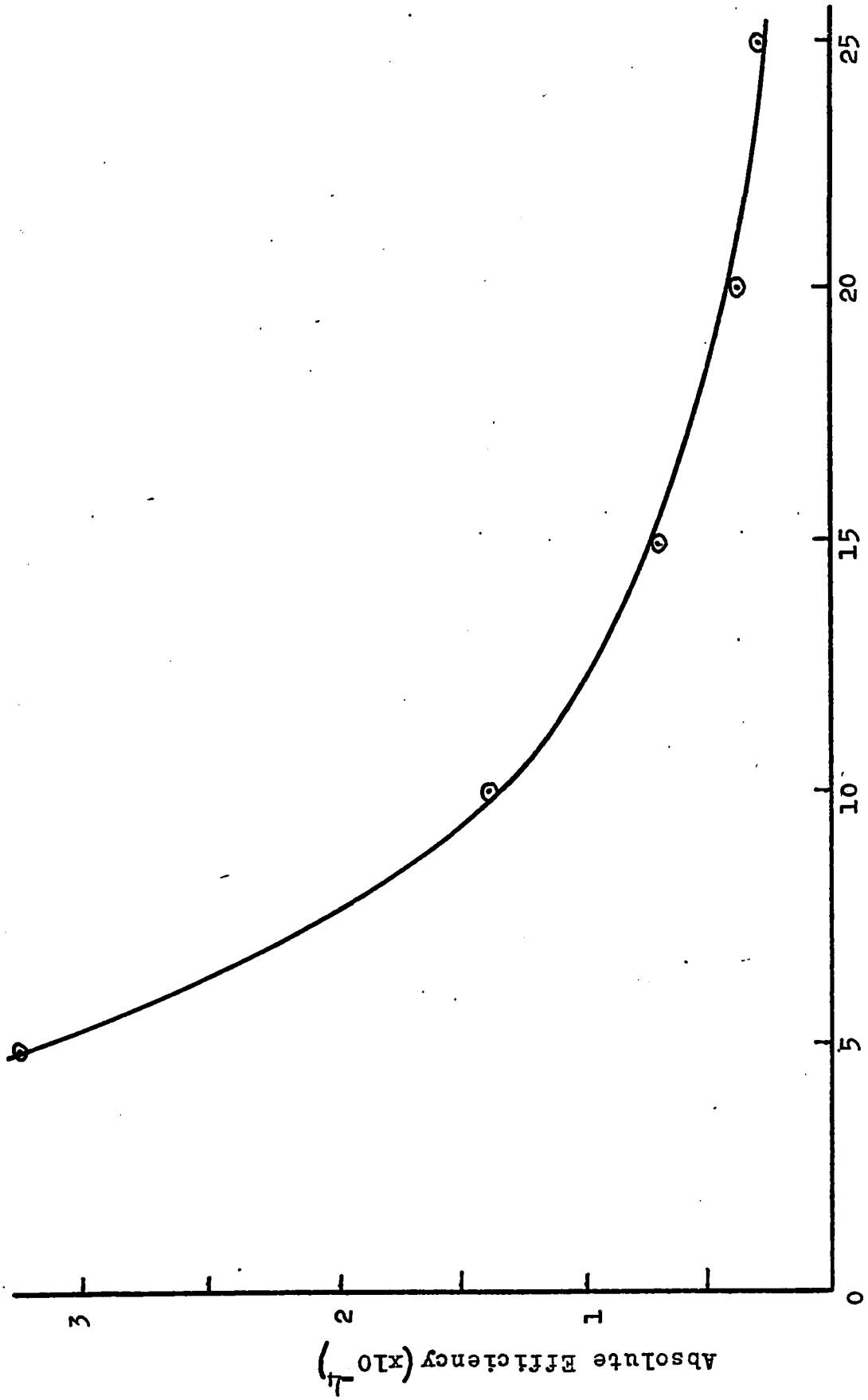

Figure 1a. Source to detector distance (cm).

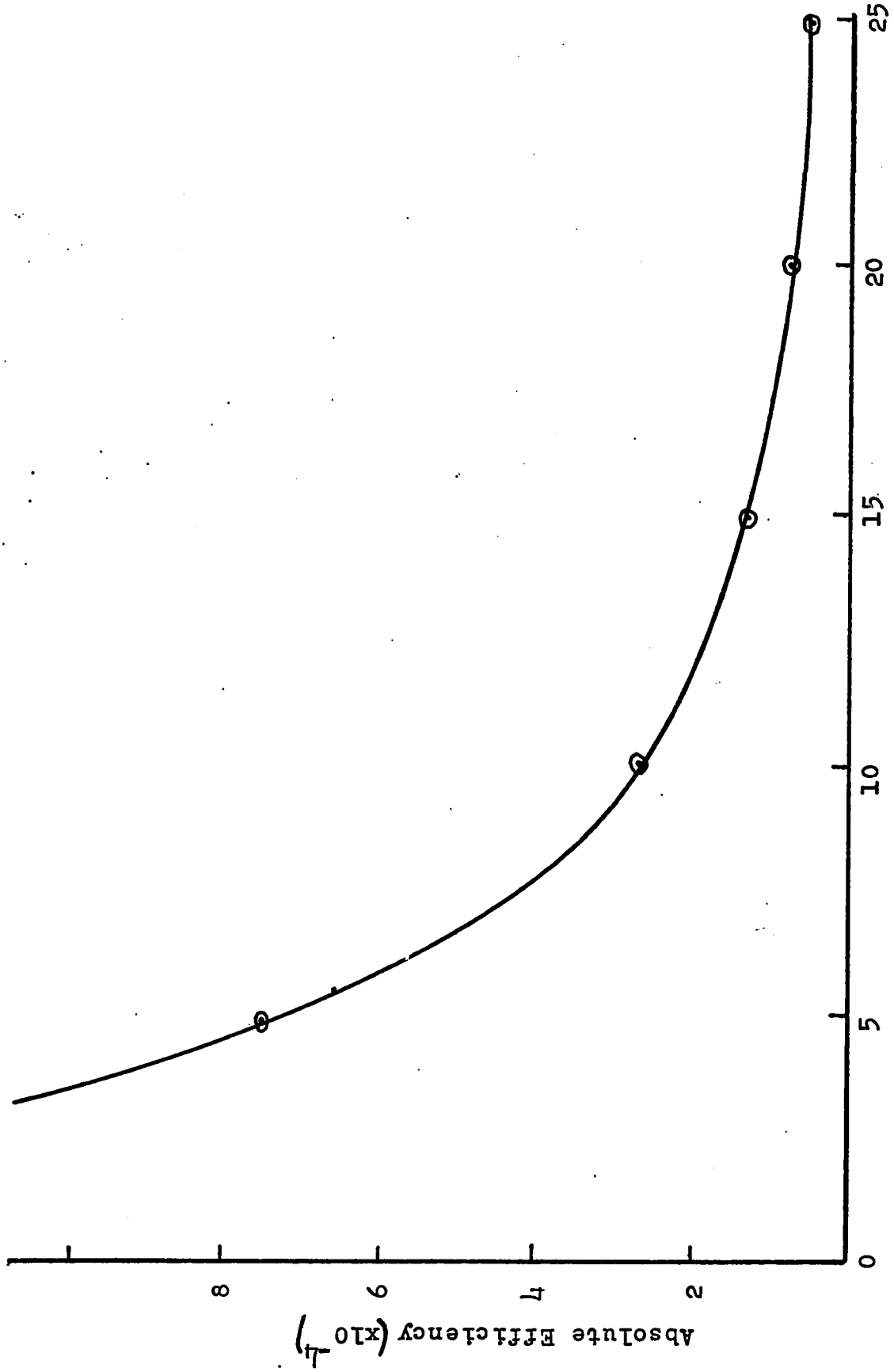

Figure 1b. Source to detector distance (cm).

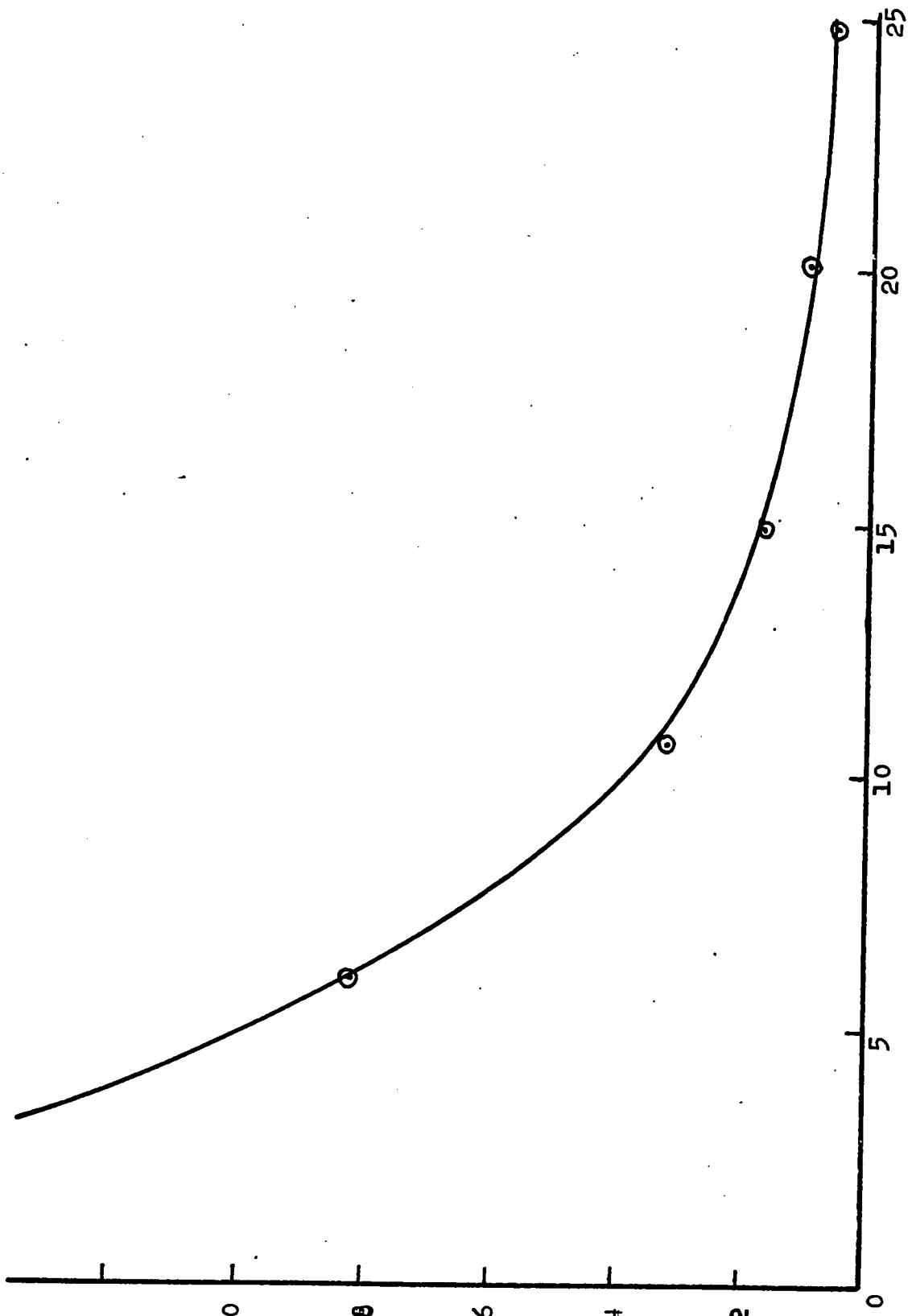

Figure 1c. Source to detector distance (cm).

Table 1

source to detector distance (cm)	Absolute efficiency of Ge(Li) detector x 10^{+4}	energy in keV
5	3.329	1333
10	1.347	"
15	0.698	"
20	0.420	"
25	0.283	"
5	6.258	662
10	2.266	"
15	1.204	"
20	0.732	"
25	0.500	"
5	7.403	122
10	2.774	"
15	1.328	"
20	0.801	"
25	0.533	"

From the above results one notes that the absolute efficiency is also a function of the energy. Errors could have been introduced by the uncertainty in the reproducibility of the source to detector geometry. The standard sources used were all encapsuled in rectangular plexiglass sheets of the same thickness, approximately 1 cm. To keep the geometry as constant as is possible, a heavy retort stand was maintained in the same position relative to the detectors, and the standard sources were always placed in the same geometry. Additional errors could have been introduced since the source-to-detector distances could not be measured very accurately due to the fact that the detectors are both sealed in containers. Probable error is approximately ± 0.5 cm

The method described above for the evaluation of the absolute efficiencies of the Ge(Li) detector was the only available one since

the strengths of the standard sources were not known. Had the strength been known beforehand then the NaI(Tl) detector need not have been used as a comparison standard and in a sense would have made calculations much easier. The procedure would have consisted of calculating the number of disintegrations per second of the standard sources at a particular geometry with respect to the detector, the Ge(Li), and then compute the area under the photopeak for the particular gamma ray desired. The ratio of these two quantities gives the photopeak efficiency of the detector at that particular geometry and gamma ray energy.

In the NaI(Tl) detector used here, the phosphor is in the form of a right circular cylinder and the source is placed along an extension of the axis of the cylinder. It has been found that a cylindrical phosphor is more satisfactory than a rectangular or cubical one, this being due mainly to the edge effects of the latter geometries. The response of the spectrometer depends on the source distance from the phosphor. The factors effecting the pulse height resolution of scintillation counters (it has been mentioned previously that the resolution of the NaI(Tl) detector is inferior to that of the Ge(Li) detector) have been reported by Prescott and Takhar. The major determinants of resolution and line shape are the statistical frequency functions of five separate processes in cascade:

a) Light production in the scintillator itself.

b) Light collection of the photocathode.

c) Production of electrons at the photocathode.

d) Collection of photoelectrons on the first dynode.

e) Multiplication in the photomultiplier dynode structure.

It was stated earlier that the photopeak efficiency of the Ge(Li) detector has been obtained via comparison with the photopeak efficiency of the NaI(Tl) detector. The actual comparison was made with the intrinsic efficiency of the NaI(Tl) detector, as defined by equation (c). These efficiencies versus energies and source to detector distances were obtained from J.H. Neiler and P.R. Bell [3] and are shown in Figure 2. The odd behaviour of the efficiency with source to detector distance is caused by penetration of the edge of the cylinder.

Usually in a NaI(Tl) detector, as the one used here, the probability that a Compton-scattered gamma ray will escape the volume of the detector is a function of the volume and will be reduced for a larger volume. Also the relative probability for total energy loss in the detector due to the occurrence of multiple events (e.g., Compton scattering followed by a photo event) will increase as the dimensions of the detector are increased.

The X-ray detector used, although also a solid state detector, does not offer as good an energy resolution as the Ge(Li) detector although it is more suitable for low energy detection. The suppliers quote a resolution of 600eV for the 14.4 keV Co^{57} gamma ray.

2.5 Electronics.

The building blocks of the electronics used in this work are the commercially available standard AEC-NIM modules purchased from Ortec, Nuclear Diodes Corporation, Harshaw and Nuclear Data Inc. The basic

Figure 2.- Calibration curves of intrinsic efficiency versus energy for various source to detector distances for the 3" X 3" NaI(Tl) detector.

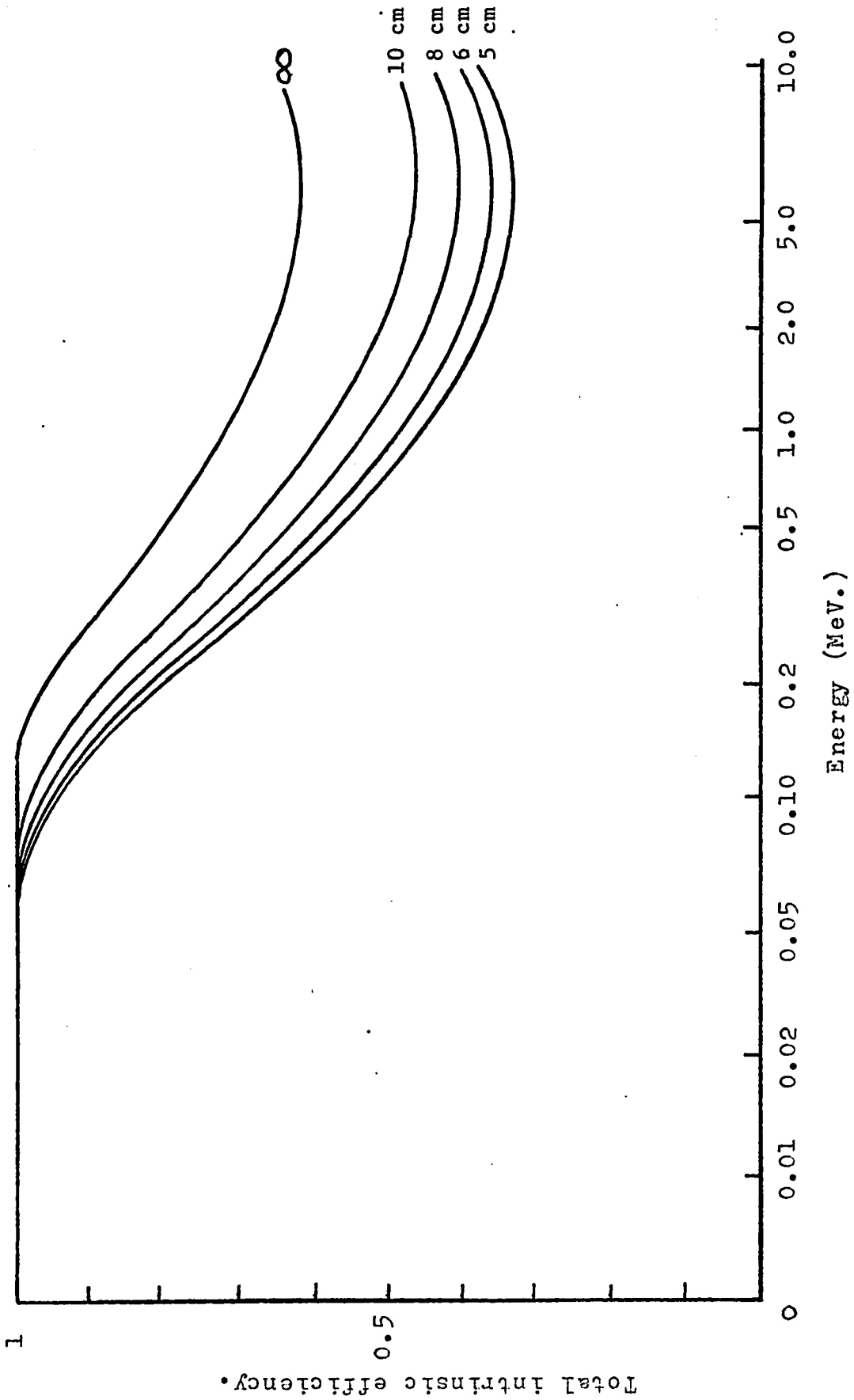
Total intrinsic efficiency.
1
0.5
0
0.01
0.02
0.05
0.10
0.2
0.5
1.0
2.0
5.0
10.0
Energy (MeV.)
∞
10 cm
8 cm
6 cm
5 cm

coincidence arrangement used here is shown in Figure 4. The resolving time of the coincidence system ranges from 10 to 110 nano-seconds.

When a pair of coincident radiations strike the two detectors, the Ge(Li) and NaI(Tl), respectively, the two signal pulses from the detectors are fed,intheGe(Li) detector case, into a pre-amplifier Nuclear Diode model 101A and from the NaI(Tl) detector directly into an amplifier, this being due to the fact that an integral component of the NaI(Tl) detector is a photomultiplier.

The pre-amplifier output consists of a step function proportional to the input amplitude, with as fast a rise time as circuit limitations permit, typically 100 nano seconds or less. This is followed by an exponential decay with a 50μs time constant. The pulse shape is often called a "tail pulse". Since the relatively slow decay requires 200μs (4 time constants) to fall within 2% of the base line, normal operation at ordinary count rates causes the pulses to pile up on the tail of the preceeding pulses. Since the amplitude is usually variable and the time occurrence is random, the preamplifier output is usually irregular. The pulse-pile-up which occurs can cause a non-linearity in the output of the preamplifier. The reduction of the preamplifier gain can reduce the pile-up effect.

All the useful information in the preamplifier output signals is included in the step function rise time and the amplitude of each pulse. These signals are then fed into a Tennelec Tc203BLR linear amplifier (from the preamplifier of the Ge(Li) detector) and a Nuclear Data amplifier model 520 (from the NaI(Tl) detector). These amplifiers

are responsible for the pulse shaping of the incoming signals and operate with time constants much shorter than the decay of the preamplifier signal and much longer than the rise time. They effectively remove the slow component that exists in a preamplifier signal and produce individual pulses whose amplitudes convey the quantity of interest, namely energy. Ideally, the pulses out of the amplifiers should not overlap so that the amplitude of each individual pulse can be accurately interpreted in subsequent measurements. However a problem does occur when dealing with high counting rates as the pulses tend to overlap one another. Other difficulties that limit the amplifier performance are input noise and base line shift. Amplifier noise is normally specified in terms of equivalent noise referred to the amplifier input. The effect of the input circuit noise depends on the choice of amplifier gain settings. In general, the amplifier noise is of least consequence when the amplifier is operated near maximum gain. An important factor, also, is the amplifier noise relative to that due to the preamplifier and this can be minimized by appropriate combination of the amplifier and preamplifier gain settings. Experiments performed with the Tennelec amplifier for obtaining the best resolution of the Co^{60} 1333 keV energy peak have resulted in the amplifier gain setting at 100. This is an important factor since the resolution obtained from the Ge(Li) detector depends also on the overall noise level that is present in the system.

Usually in AC coupled amplifier circuits there is some remaining resistor - capacitor interstage coupling network. This is a differentiating network with a time constant usually longer than those of the primary pulse shaping networks. The net effect of these undesired

differentiation in the main amplifier outputs is an undershoot in the unipolar positive pulse. If the undesired differentiation has a relatively short time constant, the undershoot will have a larger amplitude but will return to the baseline quicker. In contrast, a relatively long time constant will produce only a small magnitude of undershoot but will require a much longer time to return to the baseline. In the case of a bipolar signal, the effect of an undesired differentiation is an overshoot following the negative portion of the bipolar output signals. Thus when the counting rate in the amplifier is such that there is a high probability of a second pulse occurring before the undershoot of a prior positive unipolar pulse has returned to the baseline, the apparent amplitude of the second pulse will decrease by the amount of the undershoot present at the time of the second pulse. Since the pulses are in random distribution, the result in spectral analysis will be a smearing toward low energies in the spectrum. This problem of undesired undershoot can, fortunately, be overcome by simply adding one resistior in the RC coupling network.

This constitutes what is usually termed as "Pole Zero" cancellation. It is limited in practice by two considerations: the need for removal of low frequency noise by an additional differentiation, and by the difficulties of stabilizing the dc output level of an entirely dc - coupled amplifier.

The signal that has now been shaped by the Tennelec amplifier is fed into a single channel analyzer, (S C A) Ortec model 420. The function of the single channel analyzer is to mark the occurrence of pulses that meet certain restrictions placed on their amplitudes.

These have both lower level and upper level discriminators that can be set to refuse a certain amplitude range in the main amplifier output. The region between the lower and upper level discriminator settings is called the single channel analyzer window. Pulses whose amplitudes fall within the "window" are marked by a logic output from the SCA. It is important to note that the output from a SCA cannot be made on the leading edge of the input pulse, since the SCA must have time to determine whether the pulse meets the requirements of the upper and lower discriminator levels. The type of single channel analyzer used here is a timing SCA which produces a SCA logic output at a time that is related to the occurrence of the event. This time related output can be used for scaling and coincidence work. In the work presented here a zero crossing discriminator was used to derive its timing signal from a ipolar i put pulse; that is, each output pulse was generated when the input pulse crossed the baseline.

The NaI(Tl) signal from the Nuclear Data amplifier was allowed to enter the other timing single channel analyzer, Harshaw Model NC-15, the SCA that was used for selecting the "gate" of the desired energies for which coincidence measurements were recorded. The calibration curve of the energy window settings versus energy is shown in Figure 3.

The output from this single channel analyzer was connected to a delay amplifier, Ortec Model 427. This enabled further adjustments of the timing of the selected pulse with respect to the output pulses for the Ge(Li) detector SCA (model 420). The timing range of the delay amplifier was from zero to 4.75 micro-seconds, and the subsequent output pulses were fed into a coincidence unit, Ortec model 414A. Also the output of the model 420 single channel analyzer was connected to the

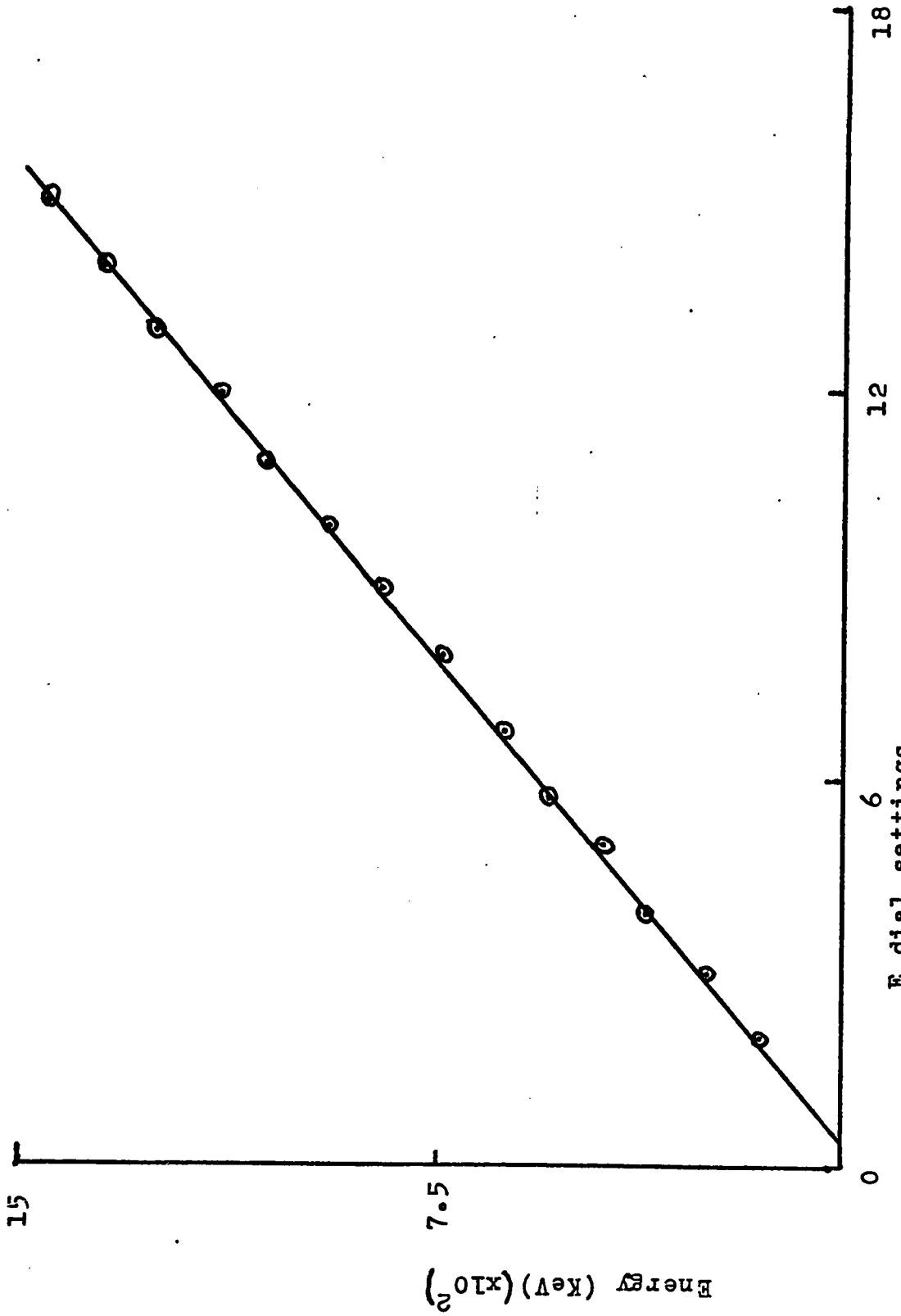

Figure 3. Calibration curve of energy window.

same coincidence unit. The function of the coincidence unit is to generate an output logic pulse when the two input signals occur within the resolving time of the coincidence unit. The resolving time range available with the above model was from 10 to 110 nano-seconds. In order to obtain this output logic pulse, the timings of the two signals that are fed into it were adjusted by means of timing switches available on each of the SCA's and the delay amplifier so that they will occur within the resolving time of the unit. In order to determine whether or not coincidence has been achieved, one of the outputs from the coincidence unit is connected to a scaler and this will be triggered for counting under the sole condition that coincidence has been achieved. One must be wary of the fact that false coincidences may also occur, and so to determine whether a true coincidence has been obtained one needs only to mistime one of the input signals with respect to the other and note whether a difference occurs in the counting rate on the scaler. If this rate has not been reduced then the only conclusion to be drawn is that false coincidence counts were taking place, if on the other hand the counting rate has drastically dropped then one can surmize that a time coincidence was obtained.

The output logic signals from the coincidence unit are then allowed to enter a gate and delay generator Ortec model 416. The output from this generator with another output form the main amplifier (Tennelec) are connected to the inputs of the analog to digital converter ADC. These two input signals must also be in coincidence before an event can be recorded in the ADC. Thus one has essentially a second coincidence unit in reference to the whole electronic system so that once coincidence has been achieved at the ADC as well, the resulting

logic pulse is stored in the memory unit from which the acquired information can be either displayed on an oscilloscope or typed on paper via a teletype. The information stored can also be transferred to a PDP-8/L computer via a direct cable. The ADC essentially converts a pulse amplitude into a pulse train whose number of pulses is a measure of the amplitude and thus allows the sorting of the pulses by digital equipment. The ADC used here was supplied by Nuclear Data series 2200(8192 channels). Data acquisition efficiency is enhanced by a 100 megahertz digitizing rate which significantly reduces the ADC's dead time. The digitizing oscillator is crystal controlled to ensure high long term stability. A digital zero shift selector enables the selected channel to be moved digitally to zero, automatically suppressing all previous channels. There are five toggle switches representing 256, 512, 1024, 2408 and 4096 channels, thus providing a maximum zero shift of 7936 channels. This enables the total energy range of a spectrum to be accumulated.

Now, in a coincidence, if one input is delayed by a very large time interval with respect to the other, some input counts can be expected. These counts originate from the accidental overlap in time of two completely unrelated pulses. One can calculate this "accidental" rate as follows: Suppose R_1 represents the rate (counts/second) of input pulses in channel 1 and R_2 represents the rate in channel 2 and let the resolving time of the coincidence circuit be Δt seconds. Due to counts in channel 1 the circuit will be open for a fraction f, of the total counting time, so

$$f = R_1 \Delta t$$

therefore the fraction of the R_2 pulses per second that will accidentally arrive when the circuit is open (due to unrelated pulses in channel 1), is

$$Ra = R_1 R_2 \Delta t \text{ counts/second}$$

The accidental rate in a coincidence system is the equivalent of background counting, or noise in a detector; the accuracy with which one measures a coincidence rate Rc depends on the ratio Rc/Ra. which should be of the order of unity and preferably much larger.

The limiting factors in coincidence experiments are essentially two:

a) The coincidence rate must be high enough to allow statistically significant data to be accumulated in a reasonable time interval. To increase the coincidence rate a stronger source may be used, or the solid angle may be increased, or the efficiency of the detector improved. The latter factor is fixed for a given detector.

b) The accidental rate must be kept well below the coincidence rate; this also depends on the source strength and solid angle, but also on the resolving time.

Suppose ω_1 and ω_2 are the solid angles subtended at the detectors (1) and (2), further suppose that ϵ_1 and ϵ_2 represent the respective efficiencies of the detectors. Then the "singles" counting rates are

$$R_1 = N\omega_1\epsilon_1 \qquad R_2 = N\omega_2\epsilon_2$$

where N is the number of disintegrations per unit time of the source. Assuming the efficiency of the coincidence circuit is 1 then the coincidence rate is

$$R_c = N\omega_1\omega_2\epsilon_1\epsilon_2$$

Melissinos [6] makes the assumption that $\epsilon_1 = \epsilon_2$ also $\omega_1 = \omega_2$ this would be a justified assumption if the two detectors were the same but they were not in this case then the accidental rate Ra is

$$R_a = R_1 R_2 \Delta t = N^2 \omega_1 \omega_2 \epsilon_1 \epsilon_2 \Delta t$$

Then the ratio of accidental to true coincidence becomes,

$$\frac{R_a}{R_c} = N \Delta t \qquad 1.1$$

The electronic set up required for the use of the X-ray detector is very similar to that of the Ge(Li) detector. For accumulation of the characteristic X-ray spectra of the source under study, the detector is connected to a preamplifier Simtec model P11HR/CN which is connected to a Simtec amplifier model 31. The acquired pulses are then analyzed on the multi-channel analyzer. The detector is mounted on a cryostat which is first evacuated with a mechanical pump and diffusion pump until a vacuum of 10^{-5} torr is achieved. The dewar is then filled with liquid nitrogen and approximately three hours are allowed for the system to completely cool. Then a G.E. triode ion appendage pump is switched on and the vacuum inlet from the diffusion pump are disconnected. After these required operations were performed, the detector was then ready for acquiring data under a negative bias voltage of 500 volts. In the set up for coincidence measurements, the NaI(Tl) detector along with the Nuclear Diode amplifier are replaced with the Simtec X-ray detector, preamplifier and amplifier.

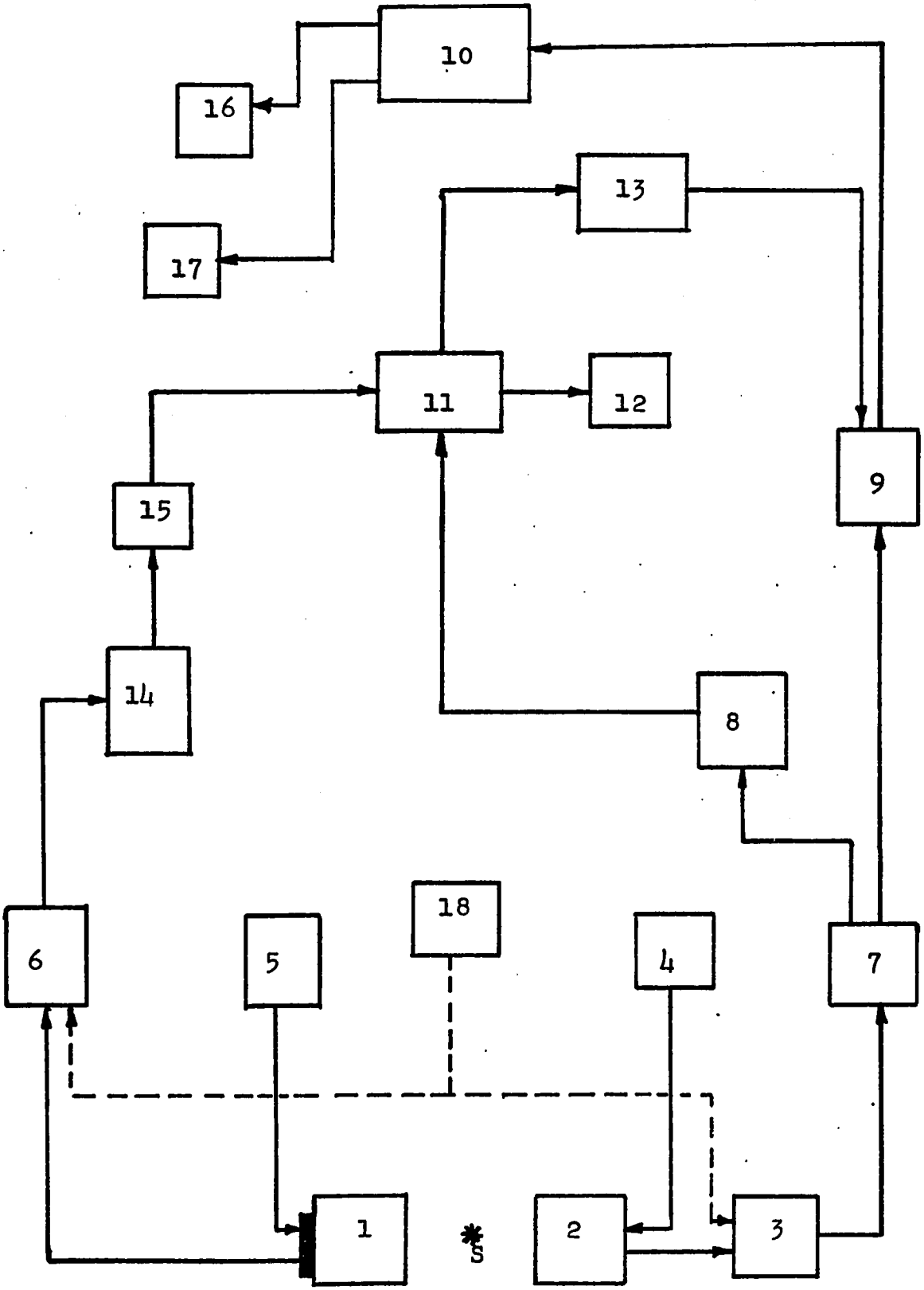

Figure 4. Block diagram for Gamma-Gamma coincidence measurments.

S - La^{135} Source

1 - NaI(Tl) detector

2 - Ge(Li) detector

3 - Pre-amplifier, Nuclear Diode Model 101A

4 - Voltage bias supply

5 - Voltage bias supply

6 - Amplifier, Nuclear Diode Model 520.

7 - Amplifier, Tennelec Tc203BLR.

8 - Single channel analyzer, Ortec model 420

9 - ADC

10 - Memory unit

11 - Coincidence unit, Ortec model 414A

12 - Scaler

13 - Gate and delay generator, Ortec model 416

14 - Single channel analyzer, Harshaw model NC-15

15 - Delay amplifier, Ortec model 427

16 - Oscilloscope

17 - Teletype

18 - Pulse generator

CHAPTER III

GAMMA RAY MEASUREMENTS ON THE DECAY OF La^{135}

3.1 History

The 19.8 Hr. half life of La^{135} was first reported by Wiener et al [1] H.A. Grench and S.B. Burson, [3] studied the $(\alpha, 2n)$ reaction on the 100% naturally abundant Cs^{133} by investigating the characteristics of the gamma rays emitted by the product nucleus and performed several coincidence measurements. The gamma ray spectra were studied by means of 2-1/4 inch cubical NaI(Tl) crystals coupled to Dumont type 6292 photomultipliers feeding into a 256 channel pulse height analyser. They observed gamma rays with energies 108 keV, 218 keV, 256 keV, 367 keV, 375 keV, 481 keV, 587 keV 640 keV and 865 keV. They also observed a strong peak at approximately 180 keV which they attributed to strong crystal scattering of the 640 keV radiation. However, they did not perform half life measurements to investigate the origins of these gamma rays. Their proposed decay scheme will be shown later in Chapter IV.

S. Morinbu et al [2] investigated the decay of La^{135} from the (p,4n) reaction on Ba^{135} by using a 4.4 cm. diameter by 5.1 cm. NaI(Tl) crystal along with a magnetic beta spectrometer and recorded the spectra on a 256 channel pulse height analyzer. They observed new transitions of 373 keV, 633 keV, 655 keV, and 852 keV. Transitions of 265 keV and 295 keV which had been reported previously, they found to be absent. They proposed two new levels in Ba^{135} at 852 keV and 871 keV in place of the 862 keV level which was reported previously by Wiener et al [1]. They also performed half life measurements on the gamma

rays and found them to have a value of 19.4 hours with the exception of the isomeric state at 268 keV which they found to have a value of 28 days. Their proposed energy levels and decay scheme will also be shown later in Chapter IV.

3.2 Source Preparation

La^{135} was produced in the McGill syncho-cyclotron via the (p,4n) reaction on Ba^{138}. The following criteria are to be satisfied in choosing the proper proton energy for bombardment:

(i) The energy should be chosen so as to give a large enough cross-section for the desired reaction.

(ii) The energy should not be such that (p,5n) reactions are produced.

Two energies of bombardment were chosen for the subsequent spectroscopic studies on the activated La^{135}. The first set were at a proton energy of 33 MeV. This effectively is the threshhold for (p,4n) reaction on Ba^{138}. The second set of bombardments were made at a proton energy of 45 MeV. The reason being that approximately 10 MeV has to be added to the threshold energy, in order to overcome the binding energy and so obtain a better product from the reaction. It was found, as will be shown in section 3.5, that when 45 MeV was used as the proton energy for bombardment a much"cleaner" spectrum of the gamma rays was obtained. The energy of the internal proton beam has been previously calibrated against the radius of the cyclotron and this calibration was accurate only to $\pm$ 2 MeV.

From the ensuing (p,4n) reaction on Ba^{138}there are other reactions which could contribute unwanted activities. These are: -

(i) Ba^{138} (p,3n) La^{136} reaction. The gamma rays subsequent to the decay of La^{136} are well known, in fact there is but one gamma ray at 0.818KeV. This also has a much shorter half life, 9.87 minutes. This gamma ray would quickly "die off" and hence would not be observed in the singles spectrum since proper data accumulation did not begin until approximately three hours after bombardment and this represents approximately 18 half lives of La^{136}.

(ii) The Ba^{138} (p,2n) La^{137} reaction. Here no gamma rays exist at all and hence would contribute nothing to the spectrum of La^{135}.

(iii)The Ba^{138} (p,n) La^{138} reaction produces the stable La^{138} isotope and consequently emit no gamma rays after a few nanoseconds.

Additional unwanted activities could occur due to impurities that are present in the Ba^{138} isotope. This isotope was procured from Oak Ridge National Laboratories 99% enriched. Isotopic analysis done by the supplier give the following breakdown: -

Barium	atomic percent	precision
130	0.01	-
132	0.01	-
134	0.01	-
135	0.02	-
136	0.02	-
137	0.20	± 0.02
138	99.80	± 0.02

A spectrographic analysis also performed by the supplier shows that the source material contained no more than 0.05% of any other element as impurities.

Prior to making bombardments on Ba^{138} for producing La^{135}, bombardments were made on Ba^{134} 80% enriched, also purchased from the same supplier, in order to produce La^{132} via the (p,3n) reaction at an energy of 35MeV for an activation time of 10 minutes. The half life of La^{132} is 4.6 hours. The singles spectrum was obtained and through rough measurements on the subsequent gamma rays emitted, they were identified. The successful identification, within the accuracy of the measurements (± 2 keV)of these gamma rays demonstrated the feasability of performing experiments with elements which have half lives of this order of magnitude using the McGill cyclotron even after the transportation of the activated source from the McGill Foster radiation Laboratory to the Physics department of Sir George Williams University. The time to transport the activated source was on the average 25 minutes.

The Ba^{138} and Ba^{134} samples were received in coarse nitrate powder form. For each bombardment about one milligram of the isotope was placed inside a thin aluminium tube which was attached to a target holder and then placed inside the cyclotron system at a fixed radius of the cyclotron appropriate to the energy of bombardment. The bombardment time on Ba^{134} lasted 10 minutes and that on Ba^{138} lasted 30 minutes. The bombardment time on a sample is a function of the half life of that sample. The average proton beam current was $1\mu A$. The irradiated samples were then transferred on a sticky tape, thus ensuring that none of the irradiated sample was lost. This tape was then suspended from a retort stand and placed at a suitable distance from the face of the detector for the subsequent studies of the gamma rays emitted. The tape suspension method of placing the source in

front of the detector was used so as to minimize the ompton scattering that may occur.

3.3 Energy Calibration and Half Life Measurements.

Prior to making any measurements on the gamma rays emitted from the irradiated Ba^{138}, it is essential to identify the energies of all the gamma rays present. For this a calibration curve of the multichannel analyzer, for energy versus channel number, is necessary. The standard sources used for the purpose of this calibration and their respective energies are shown in Table 2.

Table 2

Standard Gamma Ray Sources

	Source	Mode of decay	Photopeak energy in keV
1.	Co^{57}	Electron capture	1. 122 2. 136
2.	Co^{60}	Electron decay	1. 1173 2. 1333
3.	Cs^{137}	Electron decay	1. 662
4.	Ba^{133}	Electron capture	1. 53* 2. 81* 3. 160 4. 223 5. 277 6. 303 7. 356 8. 384

* These energies were not observed and hence were not used in the calibration spectrum.

First the spectrum of each individual standard source was acquired and the channel number position of the photopeaks noted. Then a spectrum of all the standard sources together was acquired and the photopeak positions noted. An accurate calibration curve is of the utmost importance if precise and reliable results are to be obtained from the gamma rays under subsequent investigation, it is for this reason that separate and collective acquisition of the standard source spectra were made so as to ensure that no shifts in the location of the photopeaks occured in the two spectra. The collective spectrum of the standard sources is shown in Figure 5. The results obtained were analyzed by means of a least squares fit and the equations of the calibration curves were then obtained. The calibration spectra were acquired with the Ge(Li) detector.

Two energy calibration curves were necessary for the Ge(Li) detector. One for the spectra obtained after bombardment at 33 MeV and the other when the bombardment energy used was 43 MeV because the electronic settings were altered for the two curves. In the first calibration curve only the Co^{57}, Cs^{137} and Co^{60} sources were used and for the second, the Ba^{133} source was added to the previous three. After the least squares analysis the resulting calibration equations obtained were:

$$\text{Calibration I} \qquad E = 6.2 + 1.54\ C$$

$$\text{Calibration II} \qquad E = 37.89 + 1.54\ C$$

where E is the energy in and C represents the channel number.

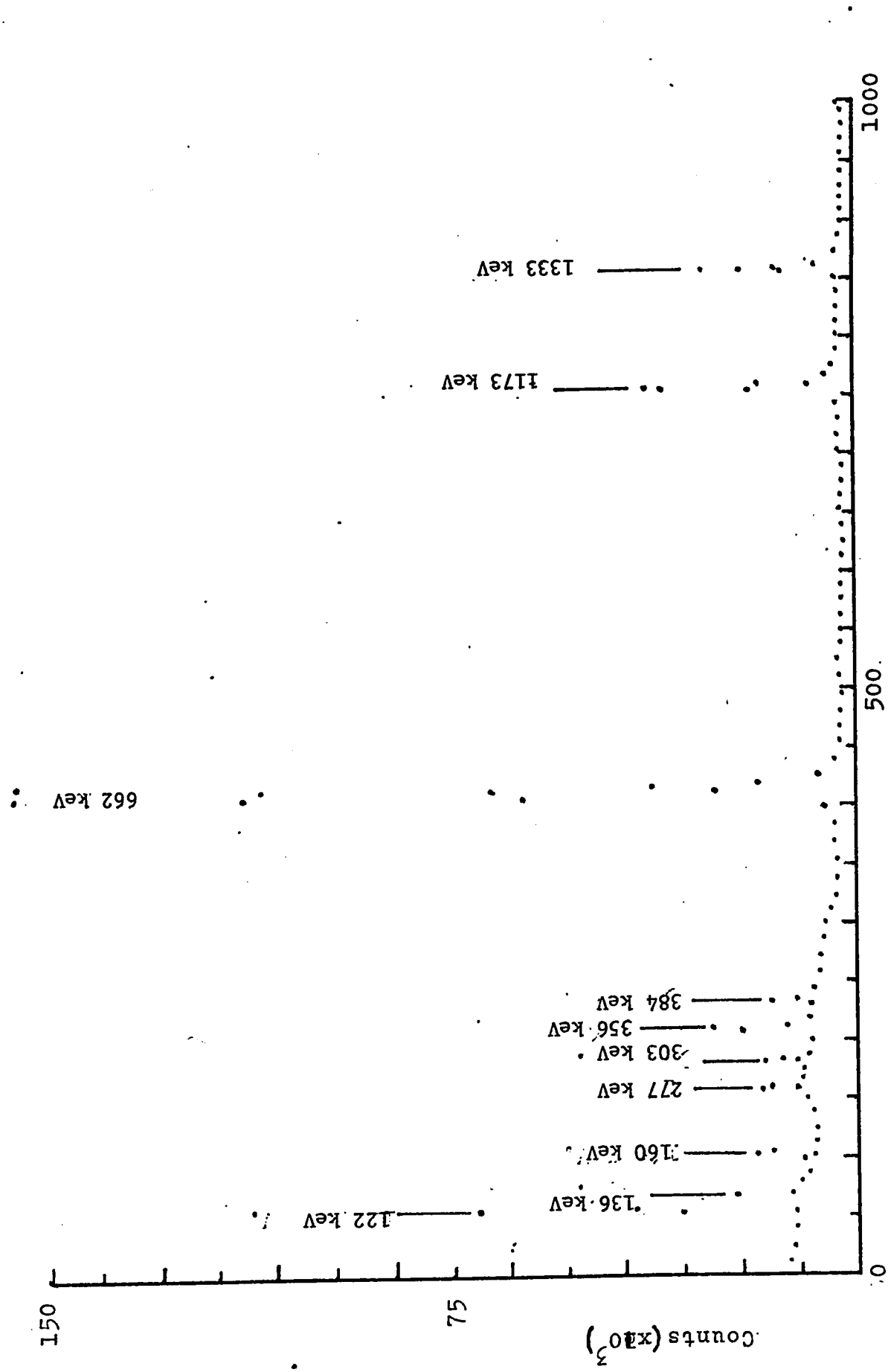

Figure 5. Calibration spectrum of the standard Gamma-ray sources.

The energy calibration of the X-ray detector was then undertaken. In the initial use of the X-ray detector problems arising from ground loop currents occurred and these had first to be resolved before any proper use of the X-ray detector. For this, three standard sources were used, namely Co^{57}, Cs^{137} and Pb^{210}, all whose characteristic X rays are well known. These are tabulated in Table 3.

TABLE 3

X-Ray calibration energies.

Source	K_{α_2}	K_{α_1}	K_{β_1}	K_{β_2}
Co	6.91	6.93	7.7	
Cs	30.63	30.97	35.0	
Pb	72.80	74.97	78.8	87.3

All the energies are in keV.

For the case of the source Pb^{210} the K_{α_1}, K_{α_2}, K_{β_1} and K_{β_2} were not observed. The reason being the Pb^{210} decays to Bi^{210} via the β^- process and emitts a gamma ray of energy 46.52 keV. This energy however is not sufficient for a K conversion electron process to occur and consequently K-X rays are not observed. What is observed are the L_α, L_β and L_γ energies along with the 46.52 keV gamma ray. The energy values of these L-X rays are well known and are given as:

L_α = 10.549 keV $\quad$ L_β = 12.611 keV $\quad$ L_γ = 14762 keV

The calibration spectra obtained are shown in Figures 6a and 6b.

The half life of La^{135} from previous investigations, has been given values that range from 19 to 19.8 hours. The main purpose of performing half life measurements was to ascertain that the desired sample was obtained after the irradiation process. The measurements were performed

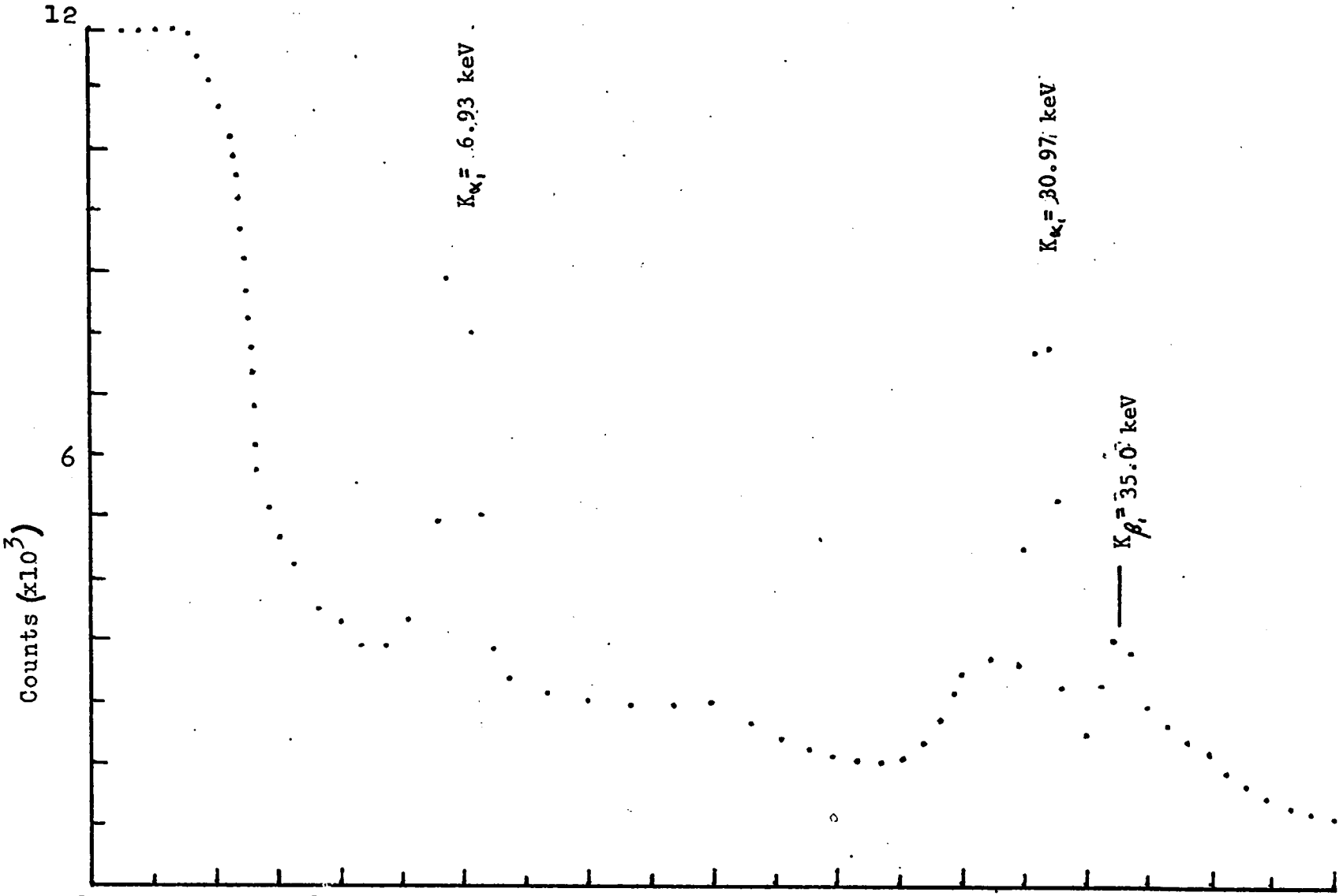

Figure 6a. X-Ray Calibration spectrum with Co^{60} and Cs^{137} sources.

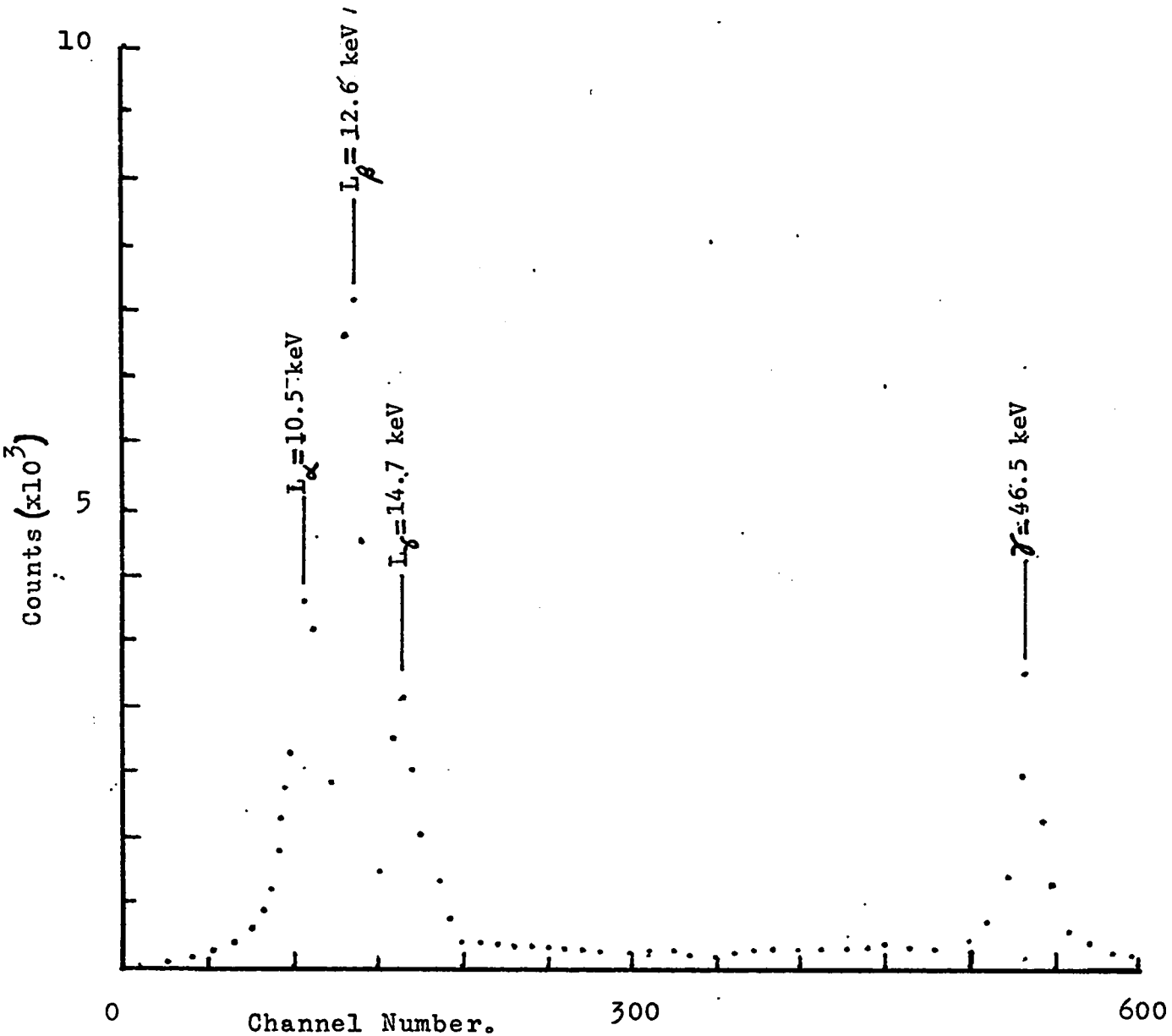

Figure 6b. X-Ray Calibration spectrum with Pb^{210} source.

on all the gamma rays observed by accumulating spectra of the active La^{135} sample for a period of 1000 seconds at intervals of 1.25 hours. The resulting data was analyzed by a least squares fitting programme from which the slopes of the linear fits were obtained for the each individual gamma ray energy peak. The curve plots were the logarithm of the maximum counts of the energy peaks versus the time interval. Strictly, one should plot the logarithm of the total counts under the area of the peak versus the time interval, but since it is assumed that the distribution of the counts is a gaussian one, the maximum peak counts or the height of the peak is proportional to the area under the curve so that the former case is sufficient. From the knowledge of the slopes obtained from the resulting linear fits, the half lives of the energy peaks were obtained. The data from which least squares analysis was done is shown in Table 4 and the resulting decay curves shown in Figures 7a, 7b, 7c and 7d. The value for the half lives was found to be 19.80 hours for the gamma rays with energies 221 keV, 366 keV, 374 keV, 481 keV, 588 keV, 633 keV, 654 keV, 856 keV and 875 keV. For the 269 keV line, the half life was found to be 28.5±0.3 hours. These results are in close agreement with the values quoted by Morinbu et al [2]. For a more accurate value for the half life, the background counts should have been subtracted from the total counts obtained in each energy peak. However, since accumulation of the spectra was only for 1000 seconds, background contribution would not be large enough to cause large errors in the subsequent evaluation of the half life value. The value obtained for the half lives of the gamma rays from La^{135} was 19.8 ± 0.3 hours.

TABLE 4

HALF LIFE DATA OF INDIVIDUAL TRANSITIONS

Energy in keV	221	269	366	374	481	588	633	654	856	875
Counts/1000 seconds (time interval 1.25 hours)	2349	3782	1001	892	6998	742	455	432	359	635
	2233	3696	995	883	6696	777	438	391	347	670
	2218	3648	963	824	6198	727	431	390	340	557
	2008	3540	901	793	6123	716	425	387	327	595
	1992	3376	854	746	5902	641	401	366	320	517
	1876	3199	823		5263	598	382	322	287	530
	1851	3027	819		5260	617	370	318	280	519
	1832	3020	787		4883	558	361	333	276	463
	1713	3009	770		4737	538	347	288	270	471

Figure 7a.- Half life curves for the 221 keV, 269 keV and 366 keV gamma rays.

Figure 7b.- Half life curves for the 374 keV, 481 keV and 588 keV gamma rays.

Figure 7c.- Half life curves for the 634 keV, 654 keV and 856 keV gamma rays.

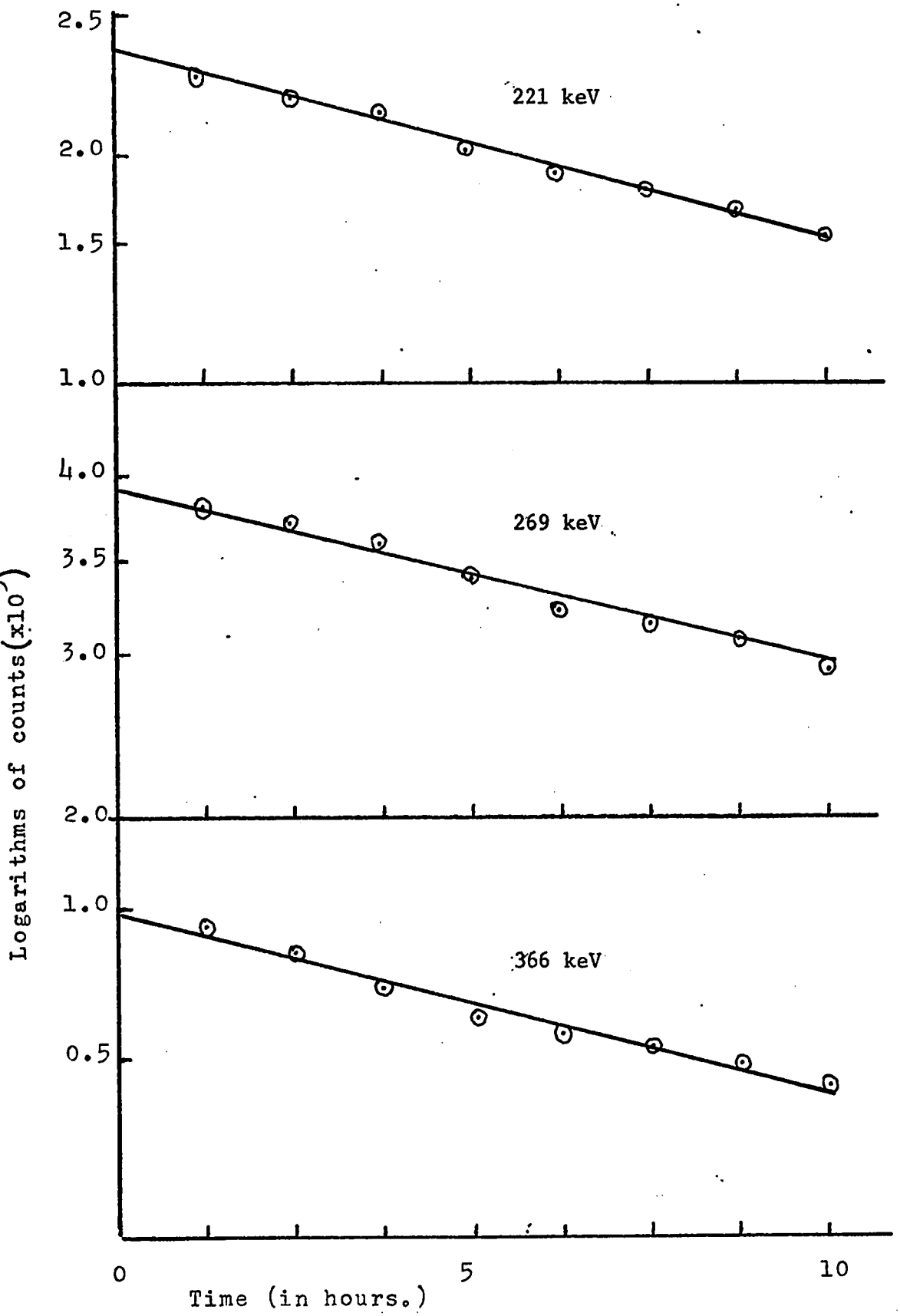
2.5
2.0
1.5
1.0
221 keV
4.0
3.5
3.0
2.0
269 keV
1.0
0.5
366 keV
Logarithms of counts(x10^3)
0
5
10
Time (in hours.)

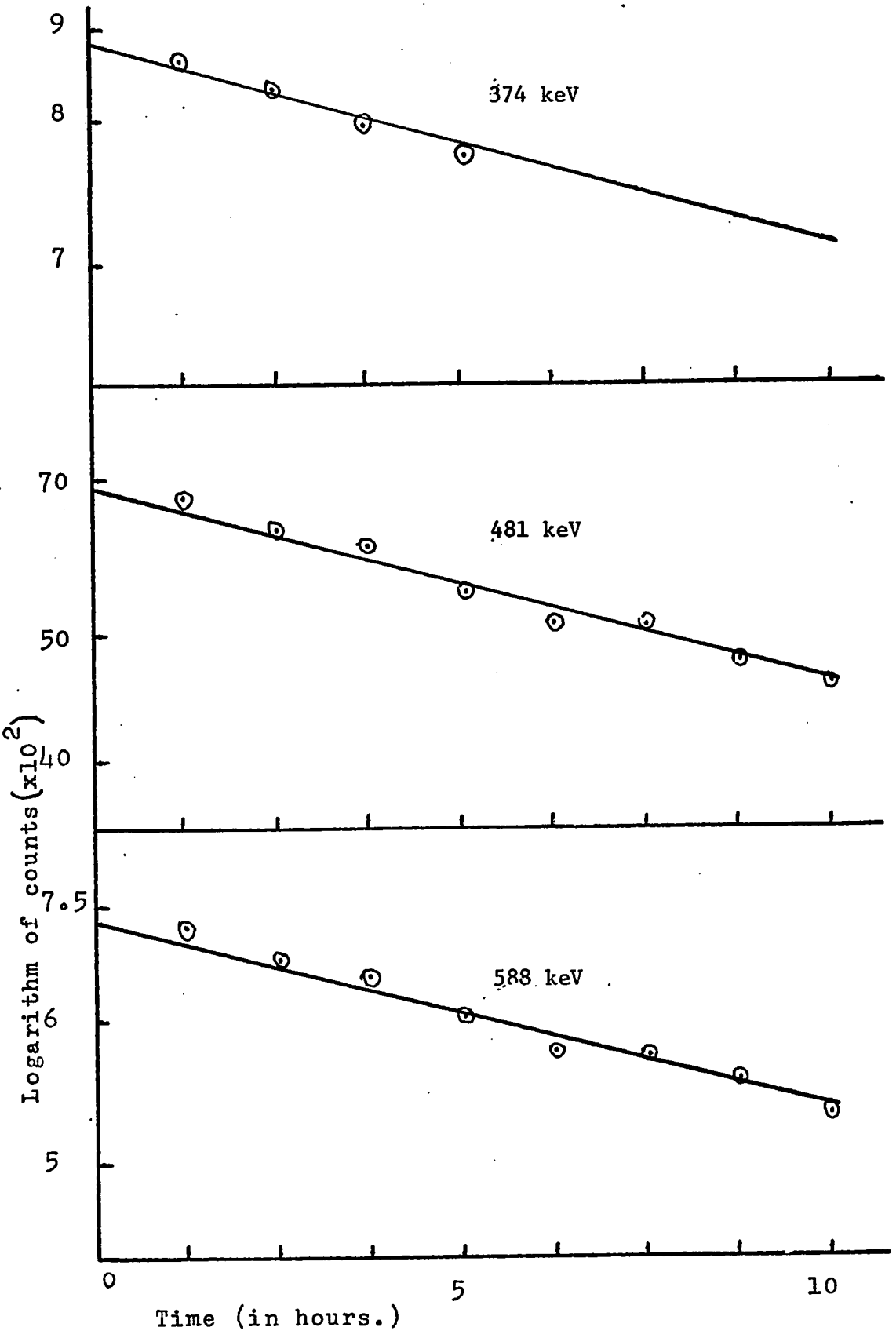
374 keV
481 keV
588 keV
Logarithm of counts (x10^2)
Time (in hours.)
9
8
7
70
50
40
7.5
6
5
0
5
10

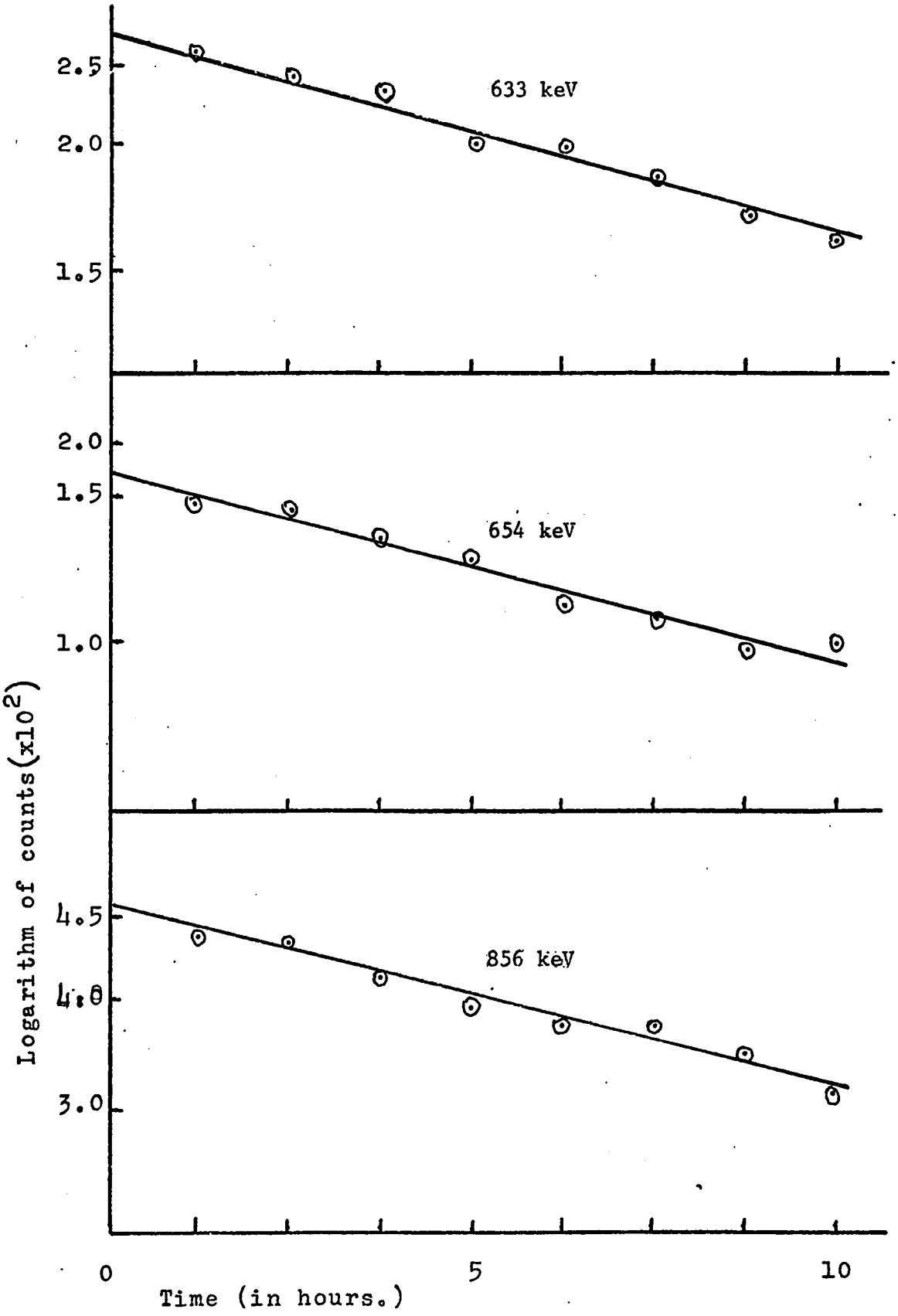
633 keV
654 keV
856 keV
2.5
2.0
1.5
2.0
1.5
1.0
4.5
4.0
3.0
Logarithm of counts (x10²)
0
5
10
Time (in hours.)

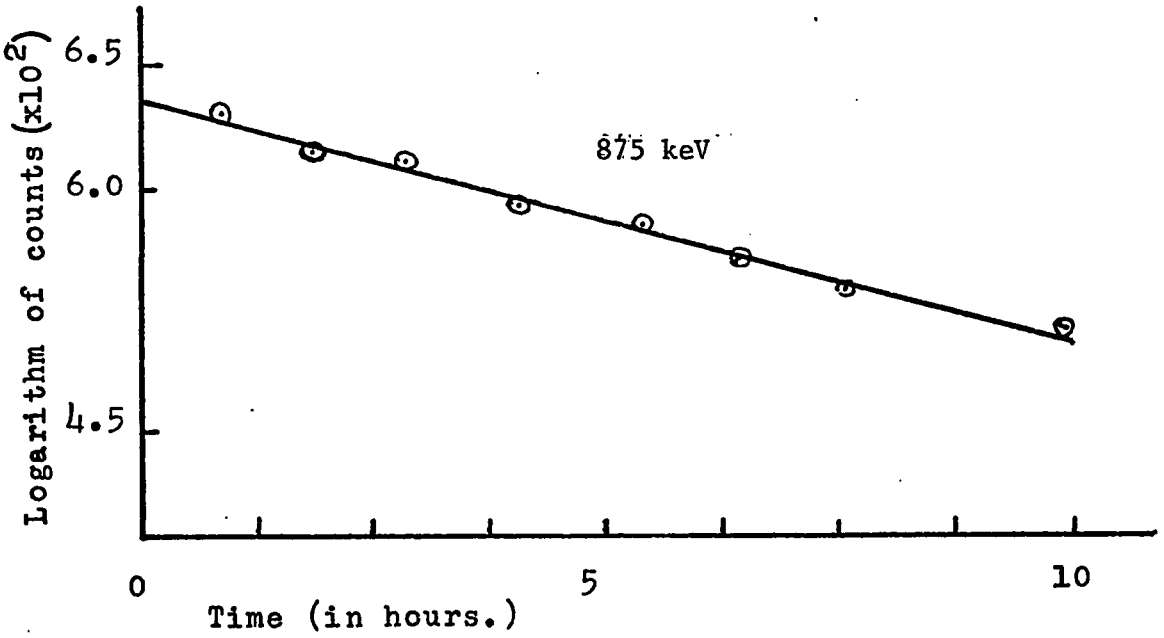
Logarithm of counts (x10²)
6.5
6.0
4.5
875 keV
0
5
10
Time (in hours.)

3.5 The Gamma Rays.

The electronic set up for singles gamma ray spectra is shown in Figure 8. The Ge(Li) detector is connected to a preamplifier which in turn is connected to an amplifier. The energy analog signals are then fed into an analog-to-digital converter. The resulting logic signals from the ADC are then stored in the memory unit of the multichannel analyzer. The stored data can be typed, via a teletype hook up, on to paper and these can then be typed on computer cards for programme analysis or the data can be transferred to a magnetic tape via a PDP-8/L computer for subsequent computer analysis. An oscilloscope connected to the memory unit enables a visual display of the spectra accumulated.

Prior to acquiring the singles spectrum of the activated sample, a background spectrum was accumulated for a period of three days. The electronic set up is identical to the one mentioned above with the exception, of course, that no radioactive source is placed in front of the face of the detector. This background spectrum is important when identifying the gamma rays emitted from the radioactive sample under investigation. The spectrum is shown in Figure 9 and the energies associated with these gamma rays, obtained by computer analysis, are shown in Table 5.

After the irradiated source was brought from the McGill Foster Radiation Laboratory to this laboratory, a certain amount of time, approximately three hours, was allowed to elapse before the actual acquisition of the desired singles spectra. This was necessary in order to allow the source to "cool" for a while after the bombardment. The

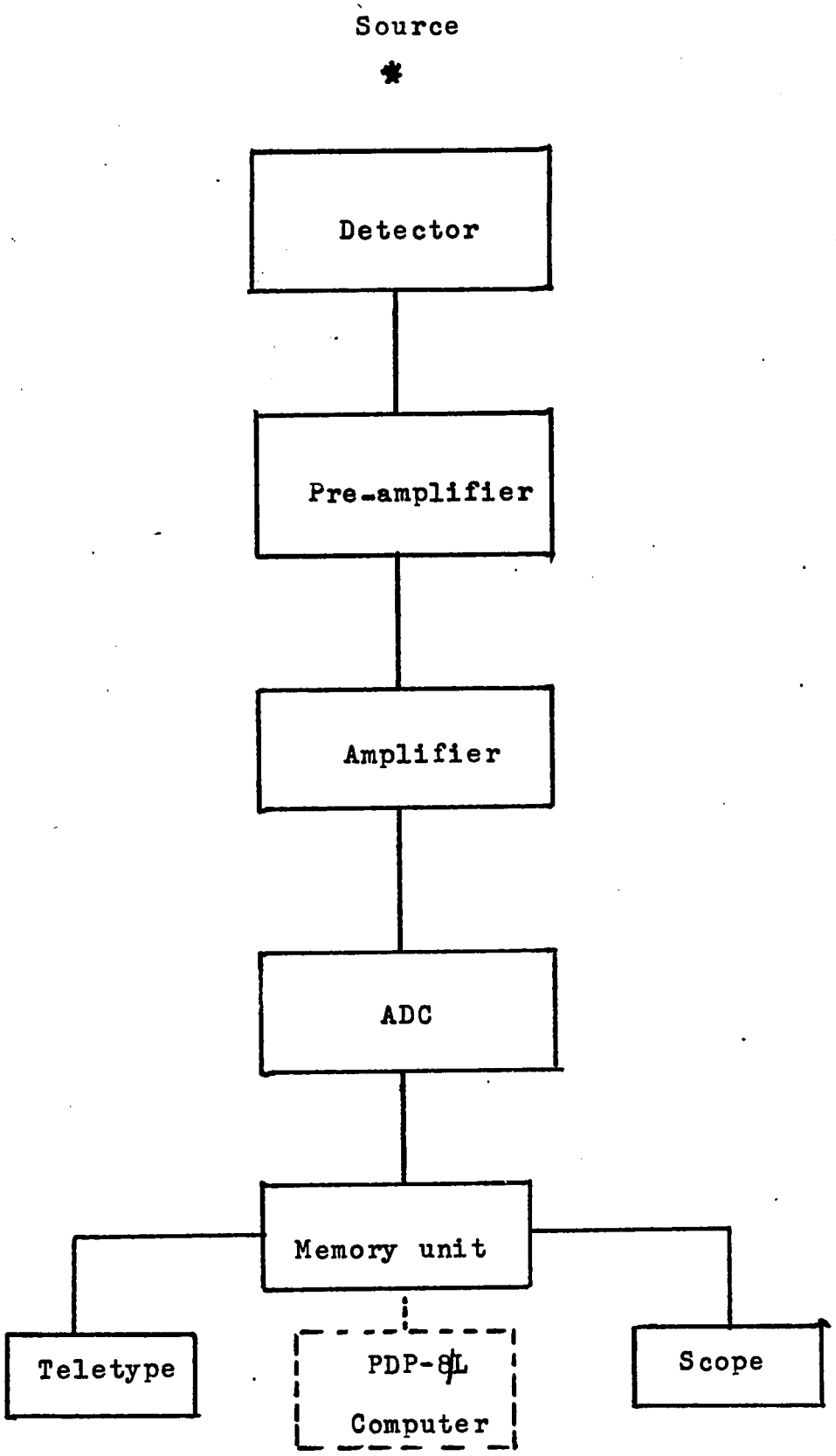

Figure 8. Block diagram for "singles" gamma ray spectrum.

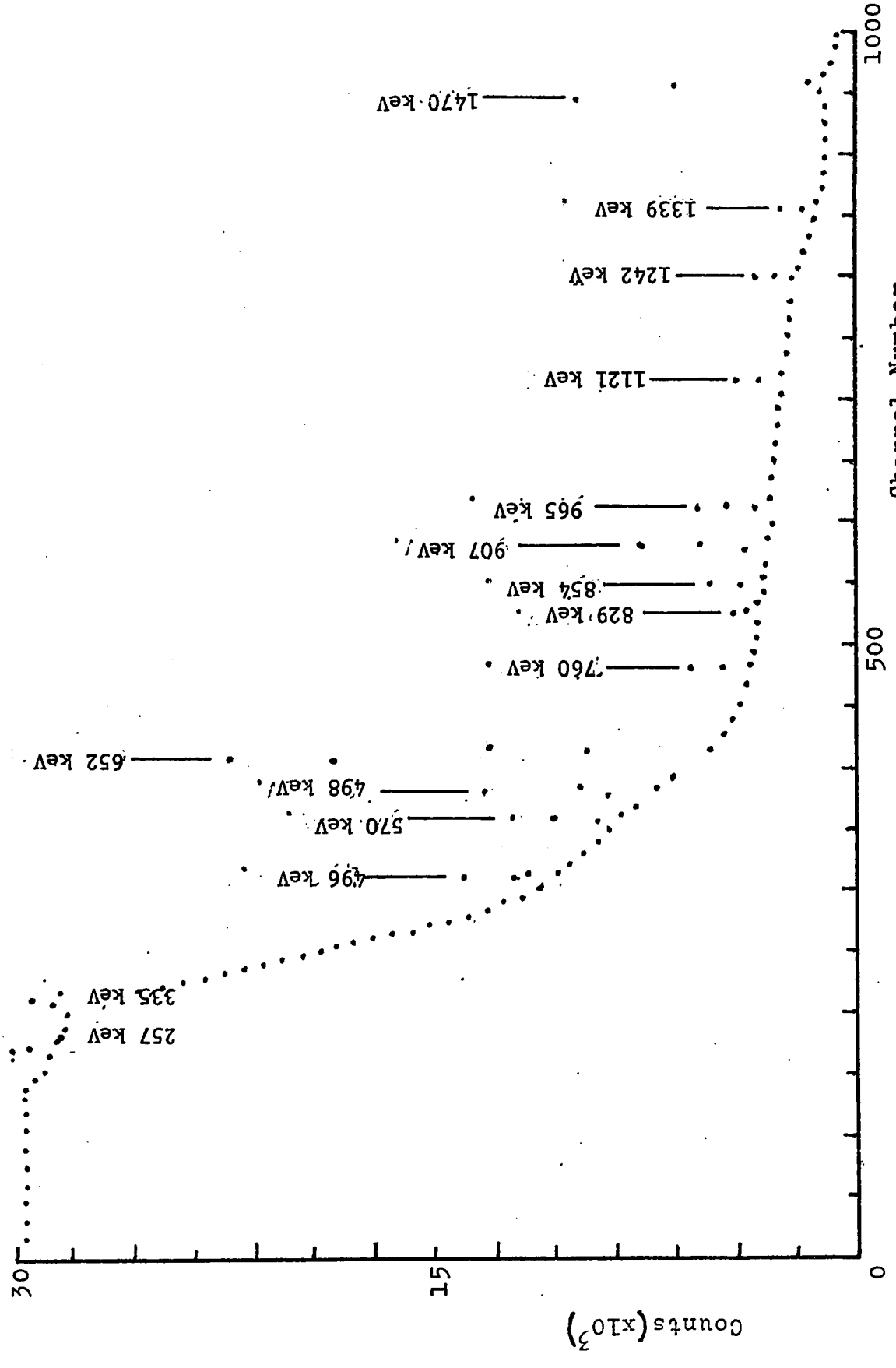

Figure 9. Background spectrum.

TABLE 5

Energies obtained from Background Spectrum.

Energy in keV (± 0.5)	Channel Number (± 0.3)	FWHM (keV) (± 0.5)	Peak counts (± 10.0)
257.0	174.5	2.3	46296.5
335.3	213.7	2.4	77007.7
496.4	318.3	2.7	37262.7
570.5	366.4	2.3	49960.3
598.7	384.7	2.5	61751.9
652.4	419.6	2.3	169840.4
760.8	490.0	5.9	5087.4
829.4	534.5	8.5	2246.4
854.9	551.1	3.5	2673.2
907.0	584.9	2.4	29411.7
965.5	622.9	3.9	15096.9
1121.5	724.2	2.6	12875.5
1242.5	802.8	7.1	7601.6
1339.1	865.5	2.6	4503.1
1470.8	951.0	2.7	267357.4

effect of a very active source can readily be observed on the Dead Time meter. This meter reads the percent of time that counts are not being registered by the electronic system. When data was acquired soon after bombardment readings on the Dead Time meter were as high as 50%, i.e. 50% of the time no counts were being registered. One method of overcoming this problem was to place the source at a large distance away from the detector, however, this geometry would have to be altered at a later time, when the activity of the source had reduced itself. This method would not be very satisfactory since it is desirable to maintain the same source to detector geometry throughout the experiment and thereby reduce the numbers of varibles that would affect the subsequent results. Another reason for allowing a "cooling off" period is that any undesirable activities that might have occurred during bombardment would have a chance to die out and so would not interfere with the desired spectrum.

The first set of acquired data of the singles spectrum was obtained when 33MeV was used as the bombardment energy on the Ba^{138} sample. The resulting singles spectra is shown in Figure 10. Computer analysis of this spectrum gave the location of the energy peaks, the FWHM and the total number of counts under each one. Using the first calibration equation previously found, (page 34), , the energies of these gamma rays were calculated. These results are displayed in Table 6. A total of twenty gamma rays were observed. The question immediately arose as to whether all these gamma rays were actually emitted from the active La^{135} sample. However, half life measurements performed on these gamma rays showed that the only ones which had half life values ranging from 19 to 21 hours were the 221, 366, 374, 481, 588, 633, 658 and 875 keV lines

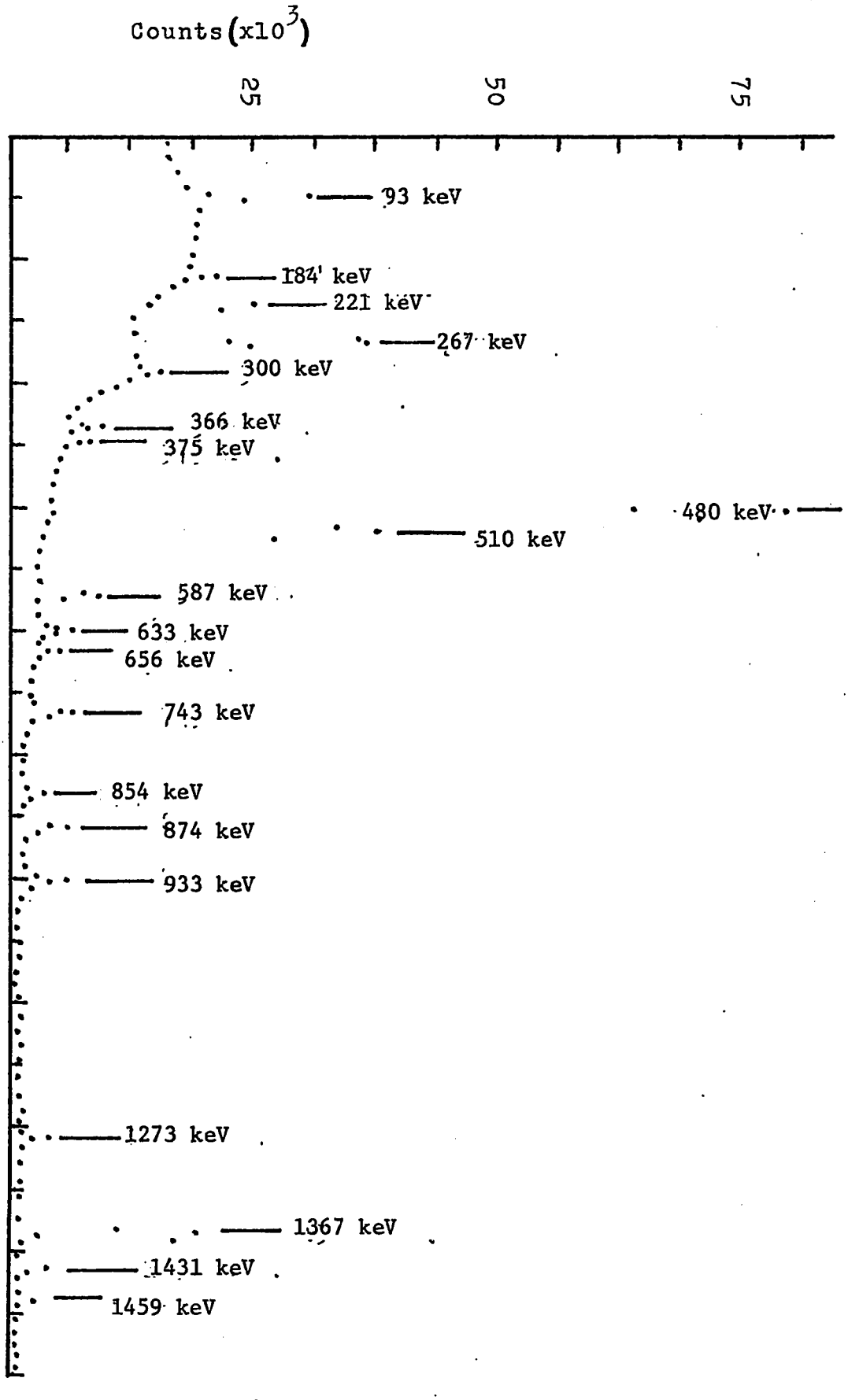

Figure 10. Singles Gamma-ray spectrum after 33 MeV bombardment energy.

TABLE 6

Gamma ray energies obtained from Calibration curve I

Energy in keV (± 0.5)	Channel Number (± 0.3)	FWHM (keV) (± 0.5)	Peak counts (± 10.0)
93.3	56.4	3.4	9178.7
184.5	115.5	2.6	27707.1
221.7	139.6	2.6	8364.7
267.9	169.5	2.6	20045.6
300.2	190.5	9.3	2175.6
366.2	233.3	4.6	1993.9
375.6*	239.4	-	-
480.0	307.0	2.8	71830.9
510.5	326.8	3.1	29029.3
587.4	376.6	3.2	4541.2
633.9	406.8	3.0	1128.5
656.0	422.5	7.6	400.6
743.9	477.8	3.9	1996.0
854.9*	550.0	-	-
874.0	562.4	3.0	3749.5
931.5	599.7	4.5	3112.7
1273.3	821.2	4.5	2530.1
1367.5	882.2	2.9	15637.7
1431.1	923.4	2.9	1189.7
1459.3	941.7	4.2	633.6

* These energies were obtained as a result of hand drawn curve fits. Error involved for the energy values is ± 1 keV

and 28.5 hours for the 269 keV isomeric state. The additional gamma rays present are thus the 93 keV., 184 keV., 300 keV, 375 keV., 743 keV, 931 keV., 1273 keV, 1367 keV., 1431 keV and 1459 keV.. In order to attempt to identify the origin of these gamma rays one has to investigate certain possibilities.

a) The choice of energy bombardment could have been such that a (p,3n) reaction could have occurred. This would produce La^{136} which Beta decays to Ba^{136} emitting one gamma ray at an energy of 0.818 MeV, also the half life of La^{136} is 9.5 minutes so that three hours after bombardment it would have undergone approximately 18 half lives, this would then make the source too weak for gamma ray detection. In fact the 0.818 MeV gamma ray was not observed. Another possible reaction could have been the (p,2n) reaction, if indeed the bombardment energy was too low. This would have then produced La^{137} which decays via beta emission to the ground state of Ba^{137} emitting no gamma ray.
The possibility of a bombardment energy too high, extremely unlikely, could have resulted with (p,5n) reaction which would have produced La^{134} with a half life of 6.5 minutes and possible gamma ray detection, after a time lapse of three hours, would have been practically impossible.

b) The ensuing products from reactions due to impurities such as Ba^{137}, which was quoted by the suppliers to be 0.20 atomic percent of the total sample after spectrographic analysis, also no more than 0.05 percent of any other element, failed to give positive identification of these "additional" gamma rays. A search for impurities through X-Ray analysis, performed in this work, has resulted in no detection of any other element other than Ba. Any impurities that might have been present were probably too small in quantity to emit energy of significant magnitude

for detection.

c) The only remaining avenue which might have led to their identification was through the half life measurements. Unfortunately these measurements were not precise enough, since high precision was not sought, to lead to positive values. Results of these measurements did show, however, that their order of magnitude was much higher than those of the gamma rays belonging to Ba^{135}. Comparing the energies of these contamination peaks with the background spectrum did not show any identifications.

In spite of the presence of all these "additional" gamma rays, coincidence measurements were performed. This will be discussed in the following section.

In order to attempt to improve the reaction product after bombardment, 43 MeV was used for the proton energy of bombardment. A marked difference was observed in the resulting spectrum as shown in Figure 11 and Table 7. It is interesting to note that the "additional" gamma rays, namely the 931 keV, 1273 keV, 1367 keV, 1431 keV and 1459 keV are no longer present. The only unidentified gamma rays still present were the 94 keV and 744 keV ones. Coincidence results, discussed in the next section, show that they do not belong to Ba^{135}. The resulting computer analysis and energy values calculated from the energy calibration curve II are displayed in Table 7. The significant difference between calibration curves I and II lies in the values of the energy intercepts, i.e. 6.22 keV for equation I and 37.89 keV for equation II. The difference is due to a slightly different lower level discriminator setting. Calibration equation II implies that no energies below 37.89 keV will be observed. This did not present any difficulties since no energies of that magnitude were expected.

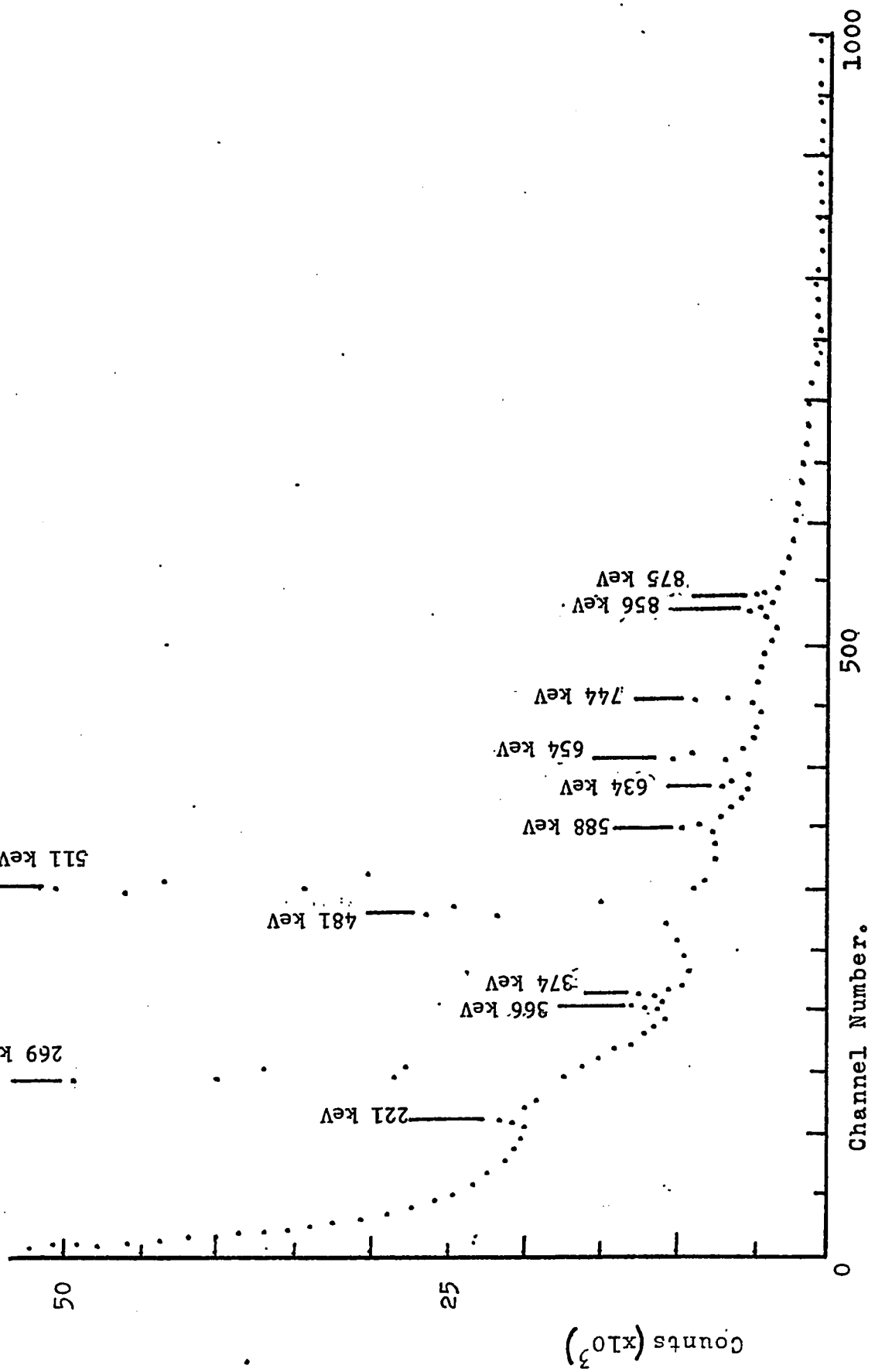

Figure 11. Singles Gamma-ray spectrum after 43 MeV bombardment energy.

TABLE 7

Gamma ray energies obtained from Calibration curve II

Energy in keV (± 0.5)	Channel Number (± 0.3)	FWHM (keV) (± 0.5)	Peak counts (± 10.0)
94.3	36.6	2.9	94178.7
221.8	119.4	4.2	26372.6
269.5	150.3	2.8	33762.8
366.5	213.3	6.0	4419.6
374.1*	218.37	-	-
481.4	288.0	3.0	196123.4
588.2	357.3	3.6	12559.4
634.0	387.1	7.5	3099.4
654.6	400.4	3.0	31530.2
744.9	459.1	3.3	16777.1
856.0	531.2	5.4	4186.2
875.4*	543.8	-	-

* These energies were obtain as a result of hand drawn curve fits. Error involved for the energy values is ± 1 keV

Also if they did exist, the electronic noise in that region would make it extremely difficult to observe. Furthermore there is very high absorption of such low energies in the aluminum cap and the dead layer of the detector, which would greatly attennate such low energy spectral peaks.

The intensities of the observed energy peaks were also found by comparing the peak height counts of each and by using the photopeak efficiency curve of the Ge(Li) shown in Figure 12 the relative intensities from the 481 keV peak were calculated. These results are also shown in Table 9.

3.4 Gamma-Gamma Coincidence Measurements.

After having observed and analyzed the gamma rays following the decay of La^{135}, the next task was to establish the sequence in which they are emitted. In these types of measurements, gamma rays are detected by two radiation detectors, in this case the 35 cc Ge(Li) detector and a 7.6 cm by 7.6 cm NaI(Tl) Harshaw integral line scintillation crystal detector. In spite of the poor resolution of the latter detector relative to the former one, it is very useful because it has a much higher photopeak efficiency. The block diagram of the electronic set up has already been shown in Figure 4 and the electronic function has been discussed in Section 2.5. Since two detectors are involved in this type of experiment, the coincidence efficiency goes as the product of the energy dependent efficiencies of the two detectors. The efficiency curves for the Ge(Li) detector as a function of source-to-detector distance have been shown in Figures 1a, 1b and 1c. Of course the variation of detector efficency with volume does

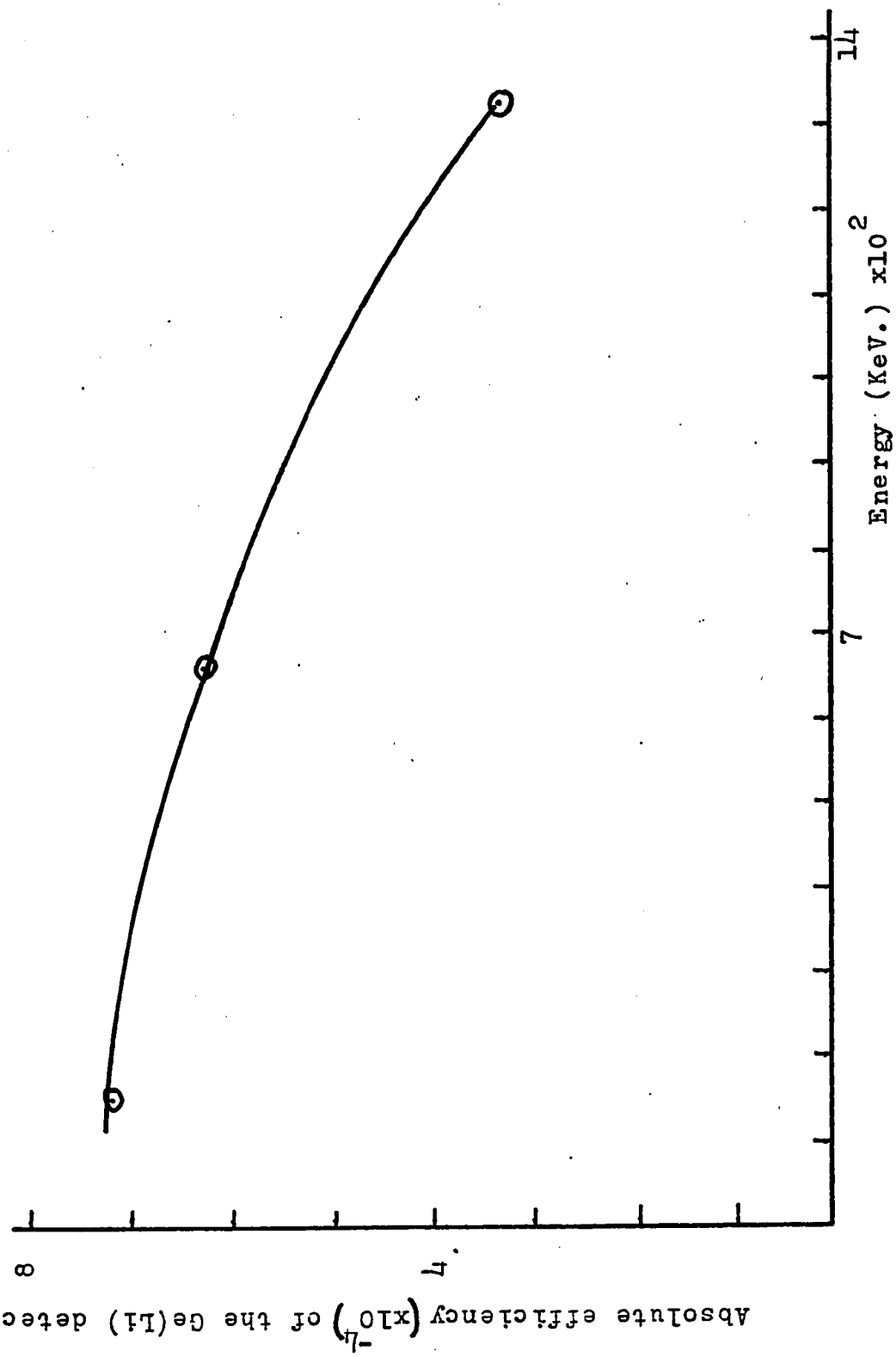

Figure 12. Photopeak efficiency curve for the Ge(Li) detector.

not come into play for a given detector. A factor which improves the efficiency of coincidence measurements is that when a selection of one of the lower energy gamma rays, in the decay scheme, as the "gate" of the coincidence system is made. However, in the study of a decay scheme, all observed gamma rays must be gated on since there is no a priori knowledge of which gamma rays are in coincidence with one another, so in this respect coincidence efficiency must be sacrificed. The consideration of the system appropriate for detecting time coincidences between pulses originating from the radiation detectors has already been discussed in section 2.5. Since short resolving times are desired, hence the rise time of the signals must necessarily also be short.

The coincidence system was first tested by using the standart Co^{60} source. This decays to Ni^{60} via β^- emission and 99 percent of the time populates the 2.505MeV energy level which subsequently cascades to the 1.333MeV level by emitting the 1.172 MeV gamma ray and in turn goes to the ground state emitting the 1.333MeV gamma ray. Therefore gating on one of these two gamma rays should result in the observation of the other gamma ray in coincidence. Use was made of a pulser Ortec Model 448. After this has been calibrated for energies, it enables the generation of pulses with prescribed energies. With this set up, the pulser essentially replaces the source and the two detectors since the generated pulses from it are fed through the two branches of the whole coincidence system, then by appropriate timing adjustments, coincidence counting is achieved. The energy calibrated pulser was then adjusted to generate pulses of 1.333MeV and coincidence counting was obtained. The pulser was then disconnected and the Co^{60} source was placed between

the two detectors (the Ge(Li) and NaI(Tl)) Coincidence counting was obtained and the 1.173 MeV gamma ray appeared in the resulting spectrum, as expected. The use of the pulser facilitated the task since gating on the 1.333 MeV peak and the timing adjustments were already very close to the required values, and so only very fine adjustments were necessary ($<0.25\mu s$). The slightest mistiming destroyed the coincidence counting. From equation 1.1 in section 2.4, the percentage ratio of accidental to true coincidence counts was found to be 1%.

Having established that the coincidence system was satisfactorily operational, coincidence measurements with the activated source were accumulated. The next task was to find whether at least the unidentified high energy gamma rays belonged to the same element. For this the coincidence gate was set on the 743 keV line, this resulted in the appearance of the 933 keV and 1431 keV lines, as shown in Figure 13. Subsequent gating on the 933 keV and 1431 keV. lines showed that all these three energy peaks are strongly in coincidence with one another, as shown in Figures 14 and 15.

The next coincidence gate was set on the 480 keV line. This is the most prominent gamma ray belonging to Ba^{135} as seen from the calculations of the absolute photopeak efficiencies. The resulting coincidence spectrum is shown in Figure 16. The presence of the contamination peaks, at reduced intensities, i.e. 933 keV , 1273 keV , 1367 keV and 1431 keV suggests that a significant amount of accidental coincidences occurred. This may have been due to the fact that the energy gate window was set too wide or that the resolving time of the coincidence measurements made with the sample obtained from the 33 MeV bombardment energy, was not short enough.

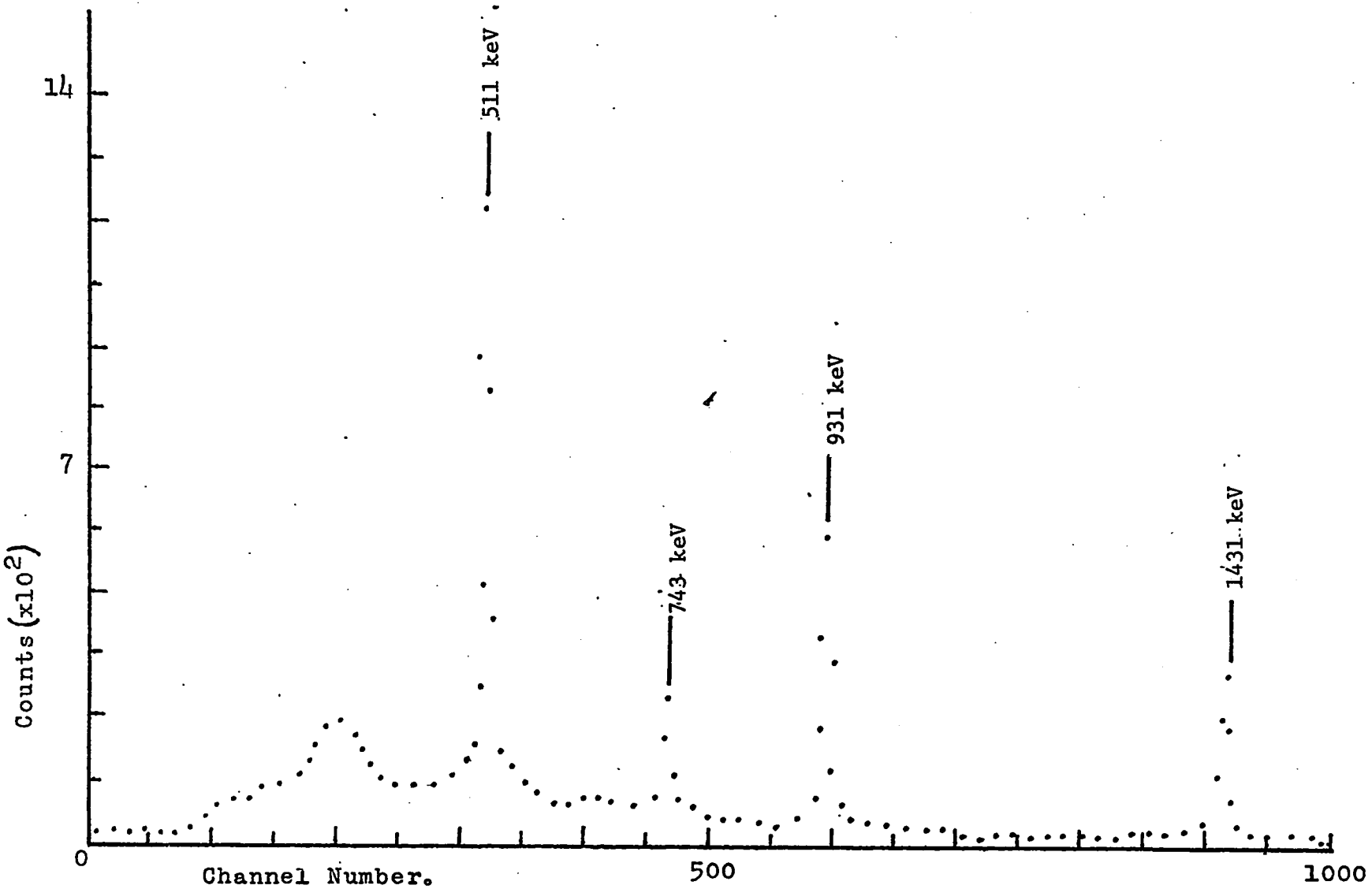

Figure 13. Coincidence spectrum with 743 KeV as gate.

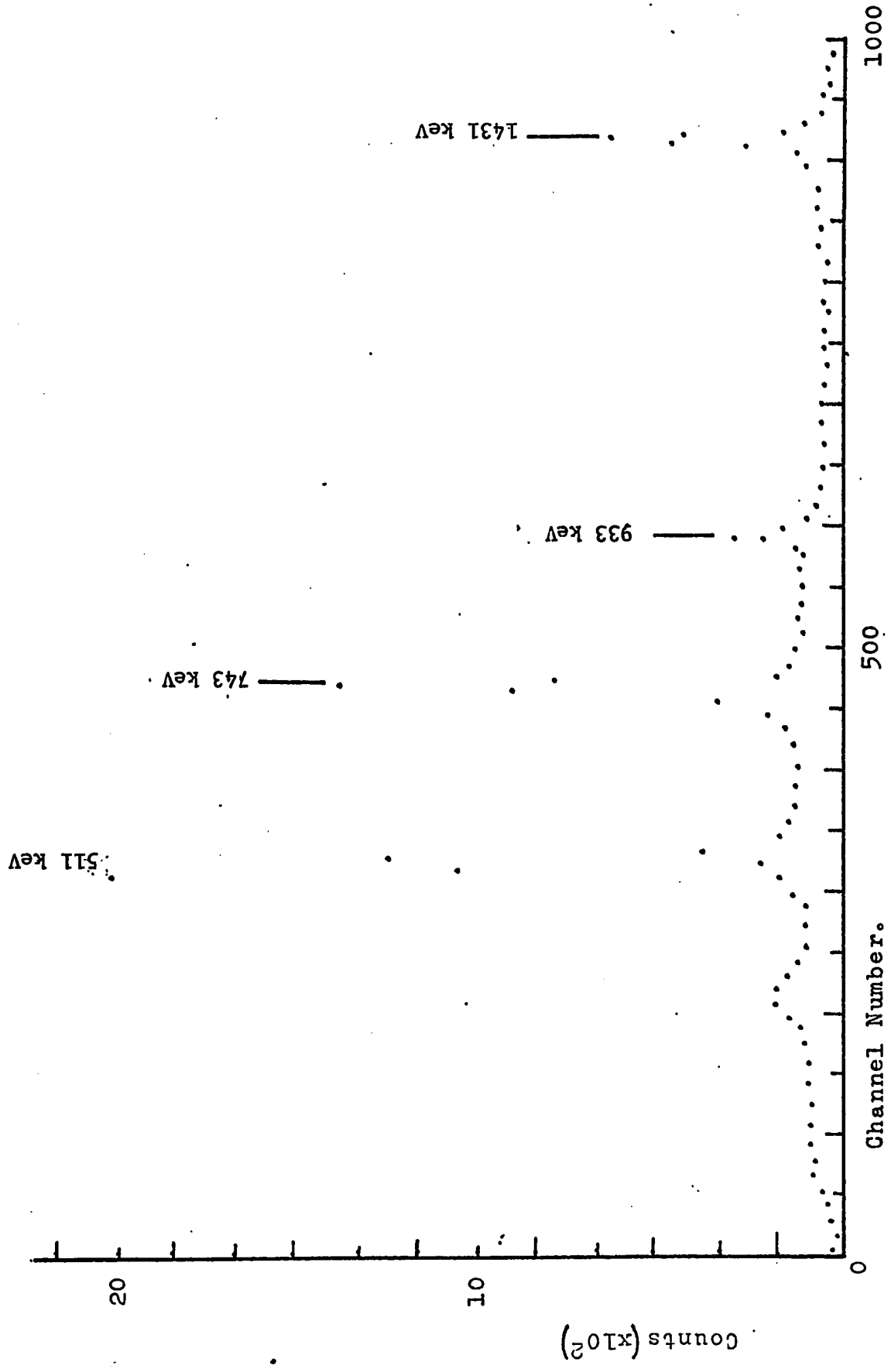

Figure 14. Coincidence spectrum with 933 KeV as gate.

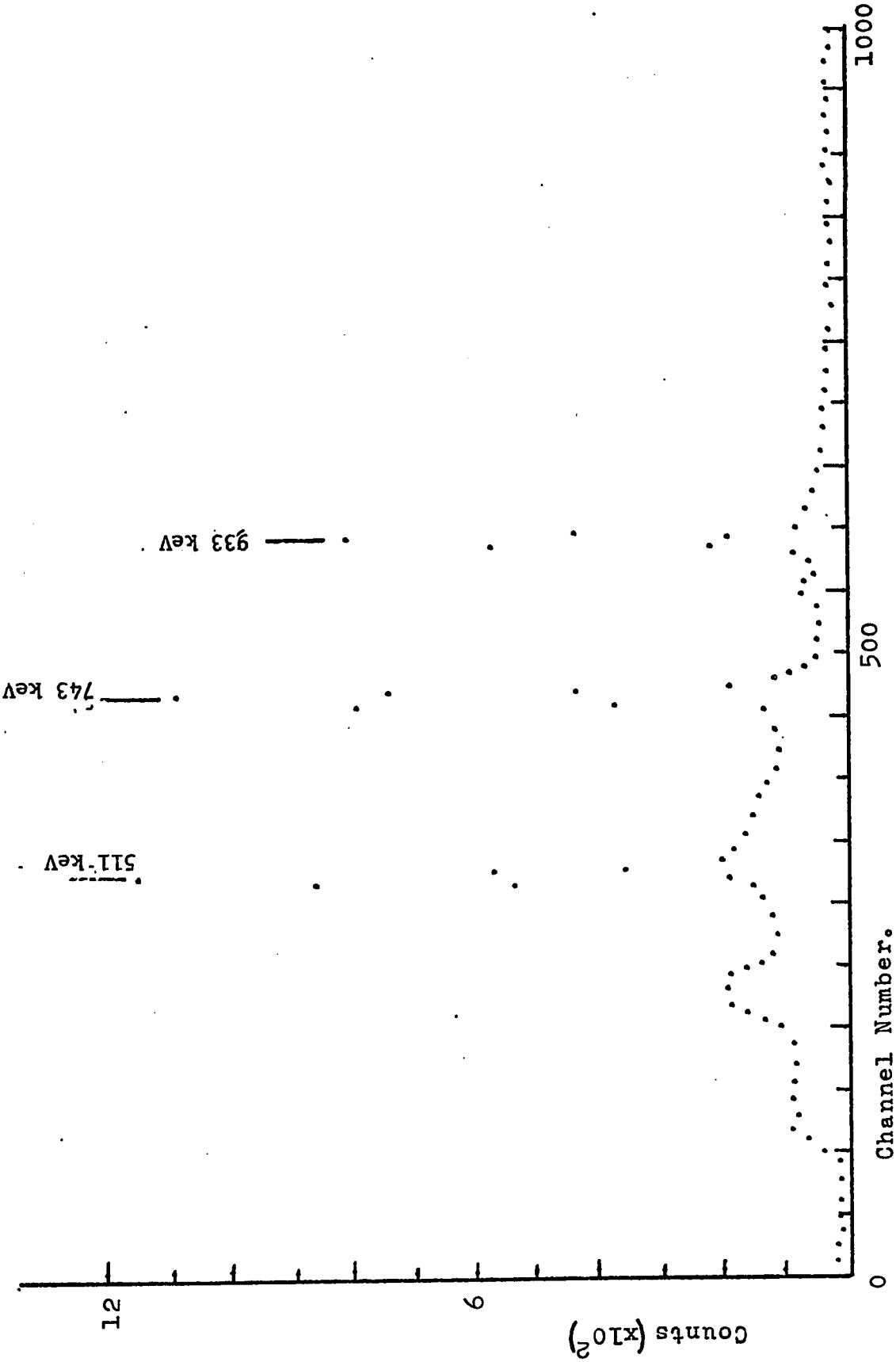

Figure 15. Coincidence spectrum with 1438 keV as gate.

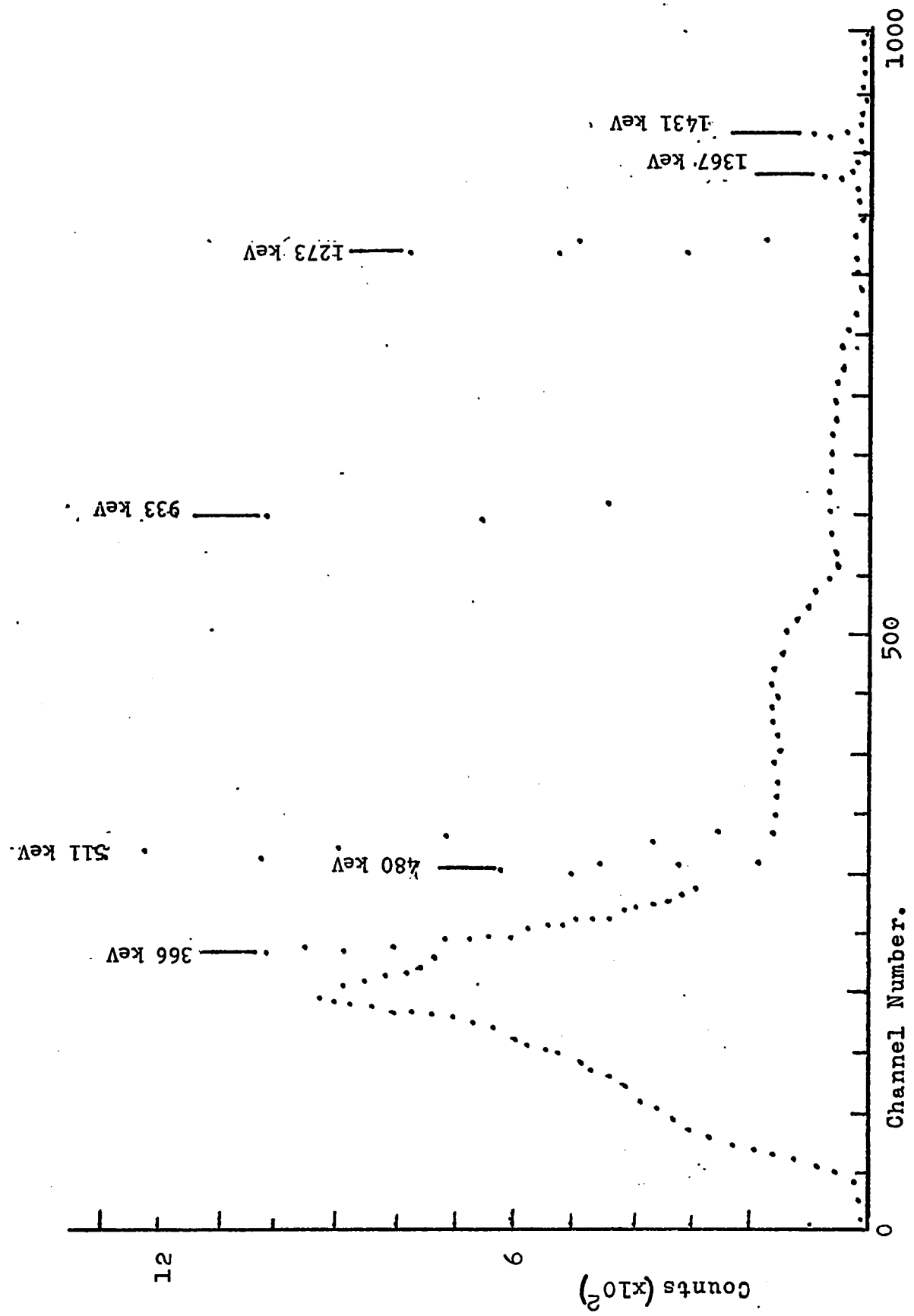

Figure 16. Coincidence spectrum with 480 KeV as gate.

When gating on the 221 keV energy peak, again the contamination peaks were observed along with the 366 keV, 633 keV and the 654 keV gamma rays, as shown in Figure 17. The presence of the three gamma rays quoted also agreed with the results of Morinbu et al.[2] In all cases of the coincidence measurements performed with this sample, the 511 keV annihilation energy has been observed, as can be seen in the coincidence spectra.

The following set of coincidence measurements were taken with the sample obtained when 43 MeV proton energy was used as the bombardment energy. As was shown in Figure 11 in section 3.5 of this chapter, a much "cleaner" singles spectrum was obtained. Consequently more readily identifiable photopeak energies were obtained in the coincidence spectra. The first energy peak which was gated on was the 481 keV and the only energy peak which was observed to be in coincidence was the 374 keV line, as shown in Figure 18. This essentially confirms the previous coincidence result and is also in agreement with Morinbu et al.[2] The gate was then set on the 221 keV peak which again resulted in the observation of the 366 keV, 633 keV and 654 keV peaks, this as shown in Figure 19. This is also in agreement with the previous results and those of Morinbu et al.[2] It is interesting to note that the 481 keV peak also appeared, at a reduced intensity. One might argue that it is in coincidence with the 221 keV line, at least partially, however, the 481 keV coincidence spectrum, Figure 18, does not indicate this possibility. Also the decay scheme systematics, as will be discussed in the next chapter, does not render this possible. A reason for this might be due to the fact that the 481 keV gamma ray is the most prominent, as regards to intensity, and is therefore difficult to "block" out.

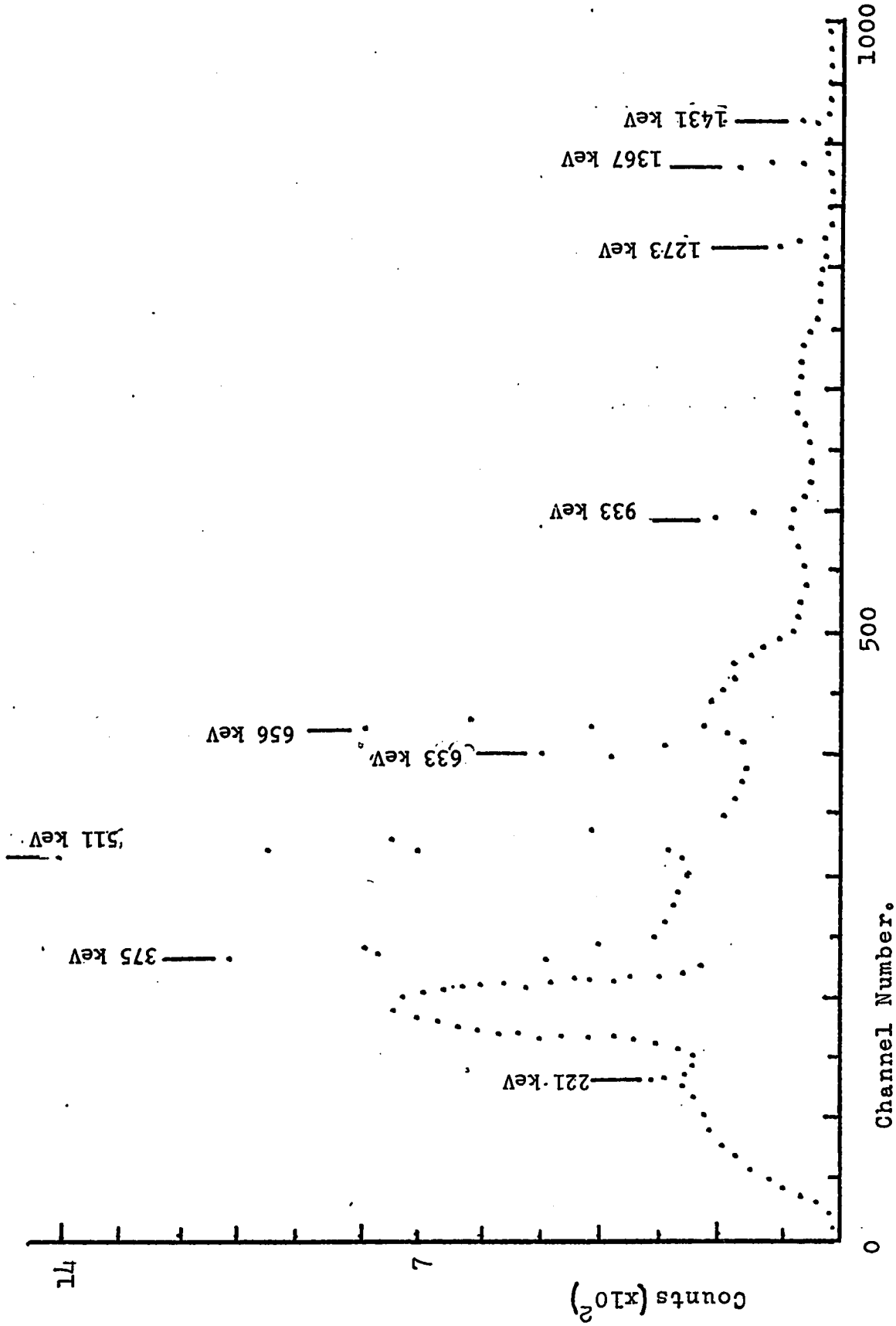

Figure 17. Coincidence spectrum with 221 KeV as gate.

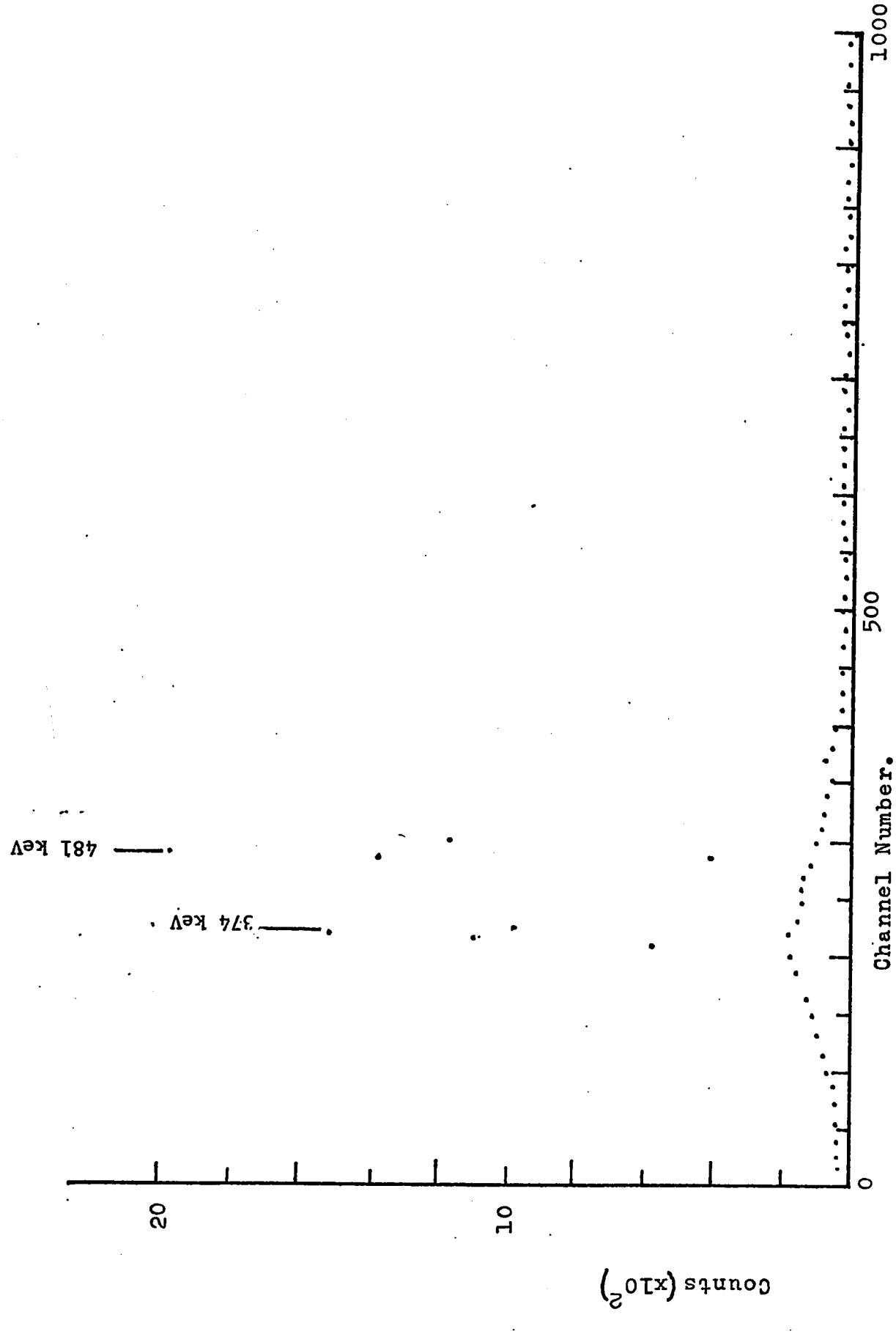

Figure 18. Coincidence spectrum with 481 keV as gate.

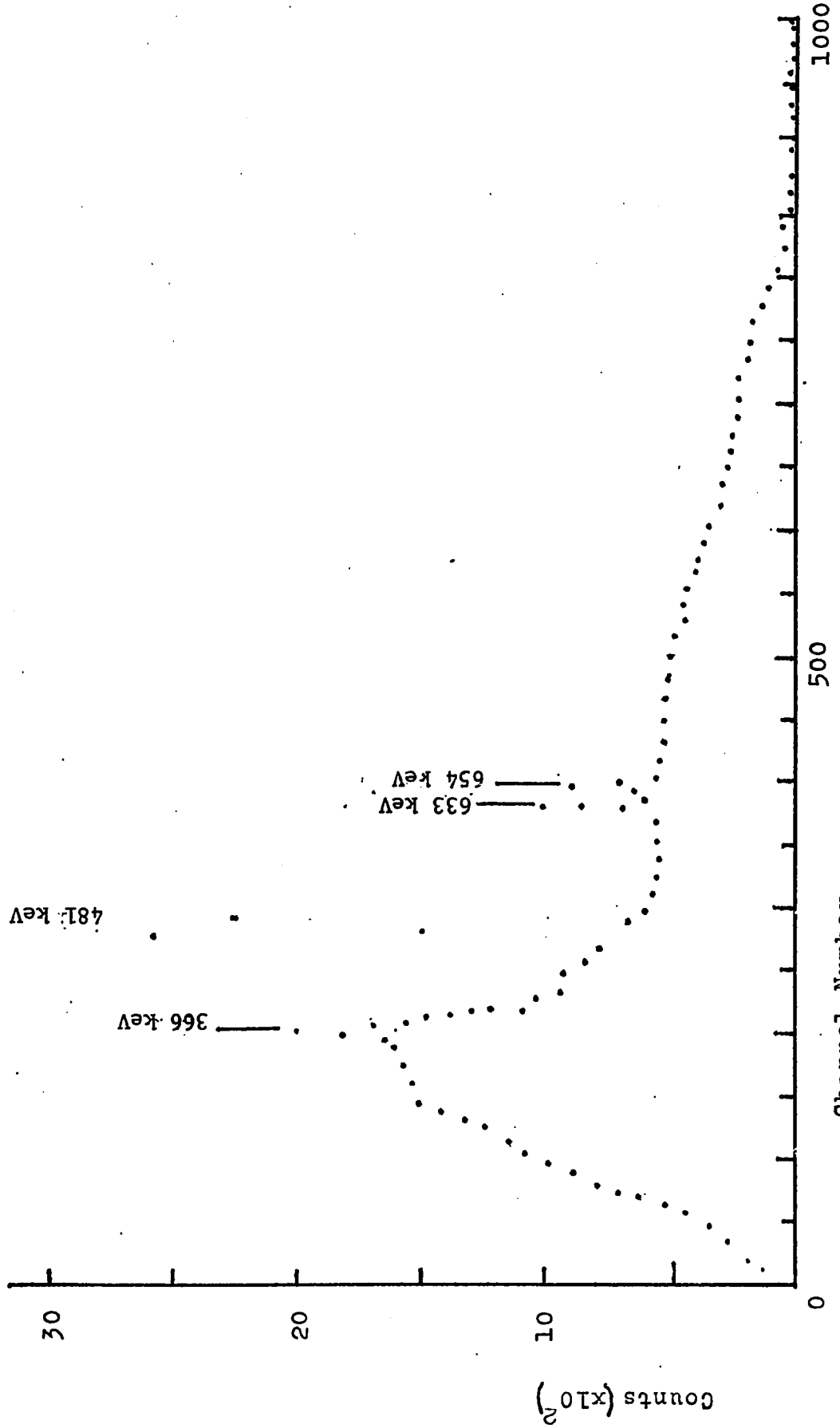

Figure 19. Coincidence spectrum with 221 KeV as gate.

Bearing in mind that

$$\frac{Ra}{Rc} \doteq 12\%$$

3.6 X-Rays and X-Rays-Gamma Coincidence Measurements

A radioactive element which undergoes an internal conversion process emits X-rays, within a time of the order of nanoseconds following the conversion electron emission, with characteristic energies of that element. X rays of varying energies are emitted depending on the transitions between different energy states. Invariably transitions to the K shell predominate and so these energies are more readily detectable. The use of the X-ray detector then makes it possible to confirm that the desired sample under investigation is in fact present and the detection of possible impurities that may be present in the sample which will subsequently give rise to undesired gamma rays. The Simtec X-ray detector along with its associated electronics, was used for this purpose. Initial experiments were performed to first eliminate ground loop currents which were present and then to find the appropriate amplifier gain settings which yielded the best energy resolution.

The resulting spectrum obtained from the active sample under investigation is shown in Figure 20. From the calibration of the detector previously performed, section 3.3, the energy peaks observed were identified to be the K_{α_1} = 32.19 keV. and the K_{β_1} = 36.40 keV. X rays belonging to barium. Since no additional energy peaks were observed hence no significant amounts of impurities can be said to have been present, if any.

In X-ray-gamma coincidence measurements one of the X-ray peaks,

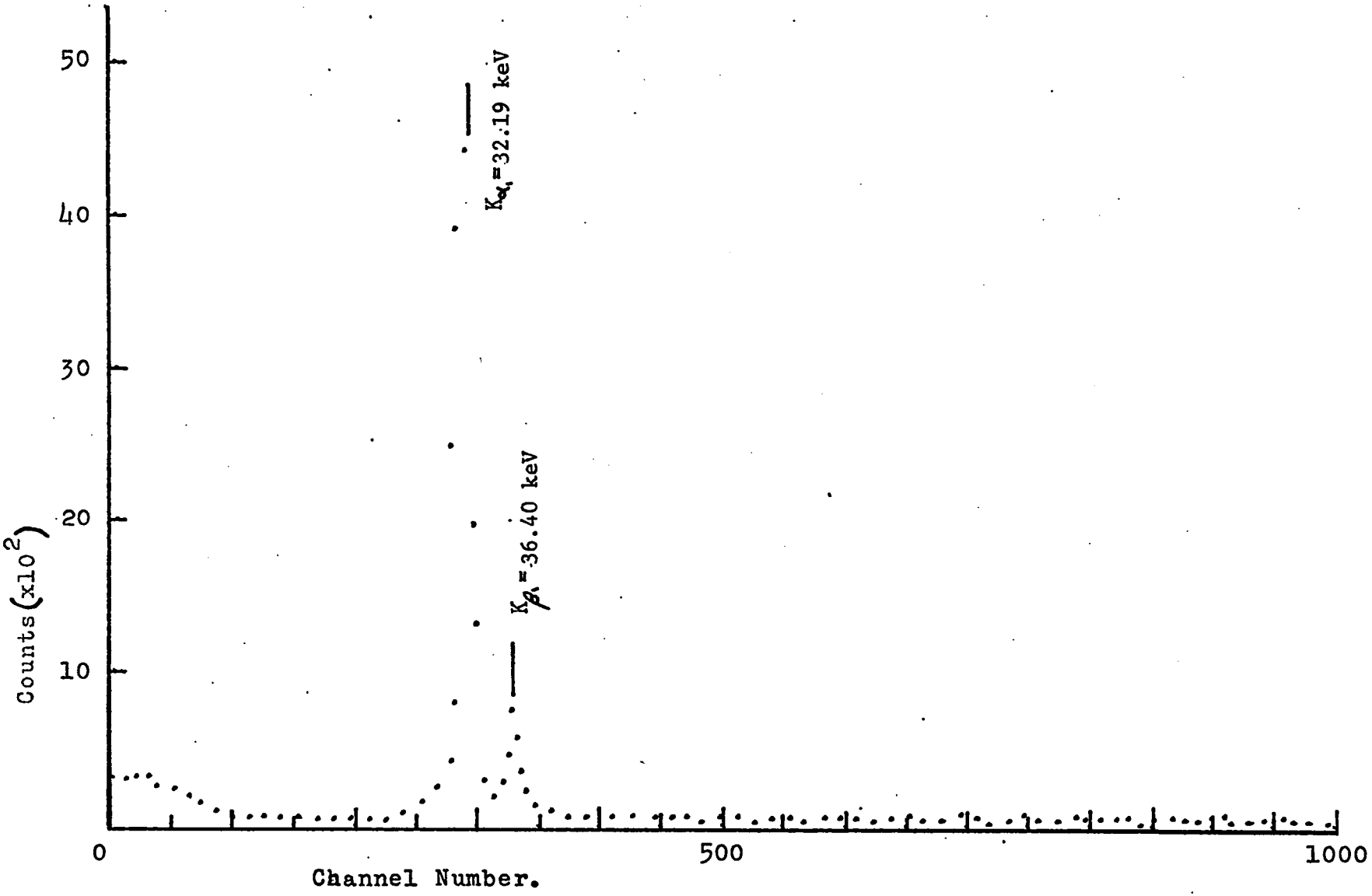

Figure 20. X-ray spectrum of Ba^{135}.

usually the predominant one, is used as the gate for the coincidence network and proper timing adjustments enables the acquisition of a coincidence spectrum involving the gamma rays, discussed in the next paragraph. The purpose of this measurement was to further substantiate that the gamma rays involved in the decay of Ba^{135} i.e. the 221 keV , 269 keV, 366 keV, 481 keV, 588 keV, 634 keV, 654 keV, 856 keV and 875 keV gamma rays are indeed associated with barium. The subsequent results can also give an insight into the extent in which gamma ray emission and internal conversion processes compete during the decay of an element.

The coincidence set up is essentially the same as the one shown in Figure 4, section 2.5, with the difference that the NaI(Tl) detector is replaced by the X-ray detector also the Simtec preamplifier and amplifier are placed instead of the Nuclear Data amplifier. The coincidence gate was set on the K_{α_1} energy peak, since it is the most intense, and after appropriate timing adjustments, the coincidence spectrum was allowed to accumulate. The resulting spectrum is shown in Figure 21. From these results it appears that all the gamma rays, quoted earlier in this section, belonging to Ba^{135} are present with the exception of the 875 keV gamma ray. Half life measurement on this energy gave a value which was the same as those of the remaining gamma rays so one cannot immediately argue that the 875 keV peak is due to contamination, also it was in the coincidence spectra. A more plausible argument would stem from the consideration of the competing processes involved in the decay. In the case of low energy excitation, the excited nucleus can decay via gamma emission or internal conversion, and, if the energy of excitation exceeds MeV, internal pair production. Internal conversion occurs if

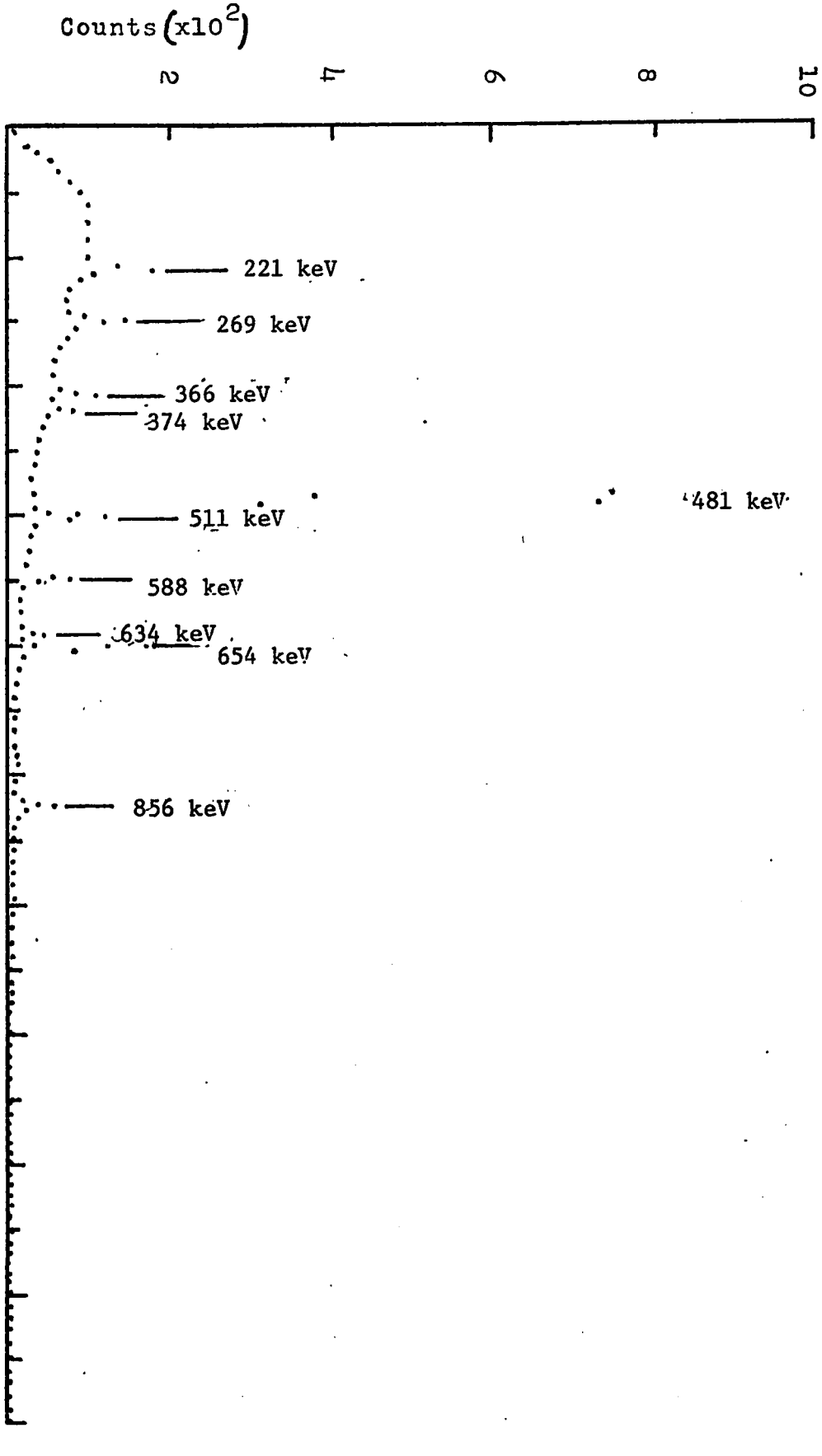

Figure 21. X-ray-Gamma ray coincidence spectrum.

the excited nucleus transfers its excess energy to one of the atomic electrons by direct electromagnetic interaction. The electron is ejected from the atom if the energy transferred exceeds the binding energy of the electron, which is usually the case except in very heavy atoms (in which the K and L shell electrons are extremely tightly bound and where the gamma rays are often low energy.) The study of internal conversion electrons comes from the study of internal conversion coefficients which relate internal conversion to gamma emission. Specifically, the conversion coefficient α is the ratio of the number of conversion electrons emitted to the number of gamma rays emitted during the same time interval. That is

$$\alpha = \frac{N_e}{N_\gamma}$$

It is also possible to distinguish "partial conversion coefficients" according to the shell from which the electron is taken. Thus,

$$\alpha_K + \alpha_L + \cdots\cdots = \alpha$$

The internal conversion coefficients depend on the character or, multipolarity, of the radiation, either $E\ell$ or $M\ell$, the atomic shell in which it occurs, the atomic number and the energy. Blatt and Weisskopf[4] give an expression for the approximate value for the internal conversion coefficient $\alpha_K(\ell)$ for K shell conversion in parity favoured transitions:

$$\alpha_K(\ell) \doteq Z^3\left(\frac{e^2}{\hbar c}\right)^4 \frac{\ell}{\ell+1}\left(\frac{2mc^2}{\hbar\omega}\right)^{\ell+5/2}$$

The above formula is a good approximation only in very special cases, namely the value of $Ze^2/\hbar c \ll 1$ and for transition energies much larger than the binding energy of the K shell electron. This formula does apply for nuclear transitions which proceed predominantly by emission of magnetic multipole radiation. Since internal conversion

and gamma emission are competing processes, no X-gamma coincidence can occur for a single transition such as the 875 keV.

CHAPTER IV

CONSTRUCTION OF THE DECAY SCHEME OF Ba^{135}.

4.1 Introduction. Energy levels and Decay Schemes.

The measurement of gamma rays is one of the principal ways of establishing the decay schemes of radioactive nuclei and of observing the levels excited in nuclear reactions. The study of gamma rays is a direct approach to energy levels since they indicate the energy separations between states. Actually the energies of gamma rays emitted from stationary nuclei are slightly smaller than the corresponding nuclear level spacings owing to the nuclear recoil effect. For nuclei which are themselves recoiling after beta-ray emission and which are moving during the emission of a gamma ray, the gamma ray energy may be raised or lowered relative to the spacing by the Doppler effect, depending on the relative angle of emission and the recoil energies. However, the errors in the direct measurement of gamma ray energies from radioactive sources are at least several orders of magnitude larger than gamma-ray recoil or Doppler shift effects. It is only when the energy level itself is used as a selective radiation detector through the mechanism of nuclear resonance fluorescence that the lowering or raising of the gamma-ray energy by beta or gamma ray nulcear recoil becomes apparent. Thus in all cases of radioactive decay the value of a gamma-ray energy obtained from a spectrometer measurement needs no recoil correction. The measured energy separation between levels connected by alpha particle emission may require a small correction for recoil associated with the alpha-particle, but Doppler shift of any subsequent gamma-ray energies is negligible.

An analysis of the transition energies as observed from gamma-ray measurements is a convenient starting point for the construction of an energy level scheme. For simple schemes consisting of only a few levels and transitions even rough measurements may be unambiguous but as the number of levels and gamma rays increase, the accuracy must be correspondingly higher. The method of analysis is based on the Ritz combination principle first employed in optical spectroscopy. Essentially, if one has three gamma rays which are thought to connect three levels and it is believed that two of the gamma rays are in cascade while the third is a cross-over transition then the sum of the first two energies must equal the third, within the errors of measurements. The intensities of the various transitions in a level scheme must also fit together in a consistant way. Thus the sum of intensities of the transitions leaving a given level and going to a lower level must equal the sum of intensities of all electromagnetic or particle transitions forming the level.

4.2 Beta and Gamma decay.

An insight of the theory of beta decay when investigating the decay schemes of elements is important since it provides some physical explanations of the events taking place during the decay, and selection rules can be developed from which assignments of spins and parities can be given to the energy levels involved in the decay.

According to Pauli's neutrino hypothesis the basic transformations involved in Beta decay are:

$$n \longrightarrow p + \beta^- + \bar{\nu}$$
$$p \longrightarrow n + \beta^+ + \nu$$
$$p + e^0_{-1} \longrightarrow n + \nu$$

Based on this hypothesis Fermi [8] gave a descriptive theory of Beta decay, from which the following result is obtained,

$$ft = \frac{\text{universal constant}}{\left| M_{if} \right|^2}$$

The product ft is called the comparitive lifetime of the nucleus. It is customery to discuss beta emission in terms of $\log_{10} ft$ instead of the ft values. Log ft values provide a simple way of comparing life times of different beta emitters, it also provides a way of obtaining information about the matrix element M. This value is also a measure of the degree of forbidden transitions. Acompilation of log ft values has been made for all known beta emitters. It is found that these values range from 3 to 20. Transitions with log ft of 3 to 6 are classified as allowed transitions, those which lie between 6 and 9 as first forbidden. For second forbidden transitions log ft is greater than 9. The quantum numbers whose change in a transition are governed by selection rules are the spin and parity. These are shown in Table 8.

In the case concerning the work presented here, the decay of La^{135} to Ba^{135} actually takes place via the electron capture process, this occurs when the probability density of the orbital electrons is high in the nucleus.

The decay of a nucleus by emission of a particle, such as an alpha or a beta particle, usually leaves the nucleus in an excited state.

Table 8

SELECTION RULES FOR BETA DECAY

Transition	ΔI	Parity Change	Log ft Value	Name of Rules
1. Super-allowed	0	no	3	
2. Allowed	0	no	3-6	Fermi
	0,±1	no	3-6	Gamow-Teller
	No o→o			
3. First Forbidden	0,±1	yes	6-10	Fermi
	No o→o			
	0,±1,±2	yes	6-10	Gamow-Teller
	No o→o			
4. Second Forbidden	±1,±2	no	10-14	Fermi
	No o→o			
	±2,±3	no	10-14	Gamow-Teller

The energy available for further decay to a lower energy or ground state is either not enough to cause an emission of another particle, or the decay by particle emission is so slow that the emission by electromagnetic interaction becomes effective. The nucleus makes the transition from the higher energy state E_i, to the lower energy state, E_f, and emits out the excess energy $\Delta E = E_i - E_f$ by means of gamma ray emission or internal conversion or internal pair production. Of these three processes, gamma ray emission occurs most often in La^{135} and in a sense, these three processes compete with one another. The gamma ray spectra, as was seen in Chapter II, consists of fairly sharp lines, showing, thereby, that the nucleus has discrete energy levels where the energy of a gamma ray emitted is given by,

$$h\nu = \Delta E = E_i - E_f$$

From electromagnetic theory, the periodic motion of the electric charges result in the emission of electromagnetic waves. Similarly the time-varying currents of a system and the motion of a magnetic dipole generate an electromagnetic wave. The emission is the result of an electromagnetic interaction between the electric and magnetic multipoles. Blatt and Weisskopf [4] performed detailed calculations for the transition probabilities, their results may be summarized as

$$\lambda(\ell) = \frac{8\pi(\ell+1)}{\ell[(2\ell+1)!!]^2}\left(\frac{\omega}{c}\right)^{2\ell+1}\frac{1}{\hbar}B\left(\ell, J_i \rightarrow J_f\right)$$

the double factorial stands for the product of odd numbers and $B(\ell, J_i \rightarrow J_f)$ is known as the reduced transition probability where the transition is from the excited state to the ground state (or to a lower excited state). Theoretical calculations of $B(\ell, J_i \rightarrow J_f)$ involves detailed knowledge of the nucleus.

Selection rules may be derived by application of different conservation laws to the system in question. The two most important conservation laws applicable to gamma ray transitions are those of angular momentum and parity.

The conservation of angular momentum requires that the total angular momentum of the initial system be equal to that of the final system. If $\bar{I}_i$ and $\bar{I}_f$ are the spins of the initial and final states, respectively, of the nuclei; then

$$\bar{I}_i - \bar{I}_f = \bar{\ell}$$

where $\ell . \hbar$ is the angular momentum carried away by a photon. One can write this selection rule as

$$(I_i + I_f) \geq \ell \geq |I_i - I_f|$$

The transition probability of pure electric and magnetic multipole radiations for excited nuclei were calculated from Weisskopf formula and it was found [5] that the transition probability, $\lambda(\ell)$, for higher multipole radiation falls off very rapidly. The exception to this rule is the $E2$ transition that is much faster than the $M1$ transition, particularly in the excited states of heavy elements.

The law of conservation of parity as applied to electromagnetic interactions require that parity be conserved. In gamma emission the system involves the parity of the initial wave function ψ_i, the parity of the final state wave function ψ_f, and the parity of the multipole radiation field. One can show that the parity change required by wave functions $\psi_i \psi_f$ are given by $(-1)^L$ for the pure electric multipole transitions and by $-(-1)^L$ for pure magnetic multipole transitions. The selection rules for different multipoles are shown in Table 8a.

Table 8a

SELECTION RULES FOR ELECTROMAGNETIC MULTIPOLE RADIATION

ΔI	$\pi_i \pi_f$	Multipoles
$0 \rightarrow 0$		(E0)
$1/2 \rightarrow 1/2$	+ 1	(E0) M1
$1/2 \rightarrow 1/2$	− 1	E1
0	+ 1	(E0) M1 E2
0	− 1	E1 M2
1	+ 1	M1 (E2)
1	− 1	E1 (M2)
2	+ 1	E2 (M3)
2	− 1	M2 (E3)
3	+ 1	M3 (E4)
3	− 1	E3 (M4)

4.3 Construction of Decay Scheme.

Before discussing the construction of the decay scheme of La^{135}, it is helpful to summarize the results obtained from measurements described in Chapter III. The eleven gamma rays identified as coming from the decay of La^{135} have energies 221.85, 269.50, 366.49, 374.18, 481.47, 588.20, 634.09, 654.59, 856.06 and 875.48keV . The 269.50keV is the energy of the isomeric state. The 374.18keV line is in coincidence with the most prominent of the gamma rays, the 481.47 KeV. The 366.49, 634.09 and 654.59 keV lines are all in coincidence with the 221.85 keV gamma ray. Electron capture results were taken from those obtained by Morinbu et al[2] who found the existence of at least five branches of electron capture decay of La^{135} to states in Ba^{135}. It is possible that other weak branches exist which were not observed due to difficulties with background. With these informations it is now possible to construct a decay scheme of La^{135} using the Ritz combination principle as discussed in section 4.1.

Considering first the coincident pair, the 374.18 keV and 481.47 keV gamma rays. There are two possibilities in which coincidence could have occurred. On addition these yield 855.65 keV.. Hence, either the 855.65 keV state feeds the 374.18 keV level or the 481.47 keV level. These possibilities are depicted in Figures 22a and 22b.

The case involving the 366.49, 634.09 654.59 and 221.85 keV gamma rays is more complicated since it offers more possible combinations. The first possibility is that they are all in a cascade. This would

involve 4! possibilities which in all cases would imply an initial level of 1877.02 keV. All of these 24 possibilities can immediately be ruled out since the mass difference between La^{135} and Ba^{135} is at the most 1160 keV. One thing can however be ascertained; that is that the 221.85 keV level is being fed from other levels emitting the other three gamma rays. Thus any combination as shown in Figure 22c is not acceptable. We then have the possibilities as depicted in Figures 22d, 22e and 22f, where in Figure 22d, γ_i or γ_j represent the 654.59 keV line, in Figure 22e, γ_k or γ_ℓ represents the 634.09 keV line and in Figure 22f, γ_m or γ_n represent the 366.49 keV line. In each of these cases we have the possibility of the existence of the following levels; 1510.43 keV, 1242 keV and 1222.33 keV. Each one of these energy levels exceeds the mass difference of 1160 keV, also none of these energies have been observed and so these possibilities can be ruled out. The remaining possibilities are those in which three of the gamma rays feed the same level which emits the fourth one. These are shown in Figures 22g, 22h, 22i, and 22j. From the schemes presented in Figures 22g, 22h, and 22i, we note the admittance that levels with energies 588.34, 856.94, 876.44, 1000.58, 1021.08 and 1289.18 keV. Any scheme which involves a level at 1289.18 keV can be ruled out since this exceeds the mass difference of 1160 keV. Gamma rays with energies of 1000.58 and 1021.08 keV have not been observed hence schemes involving these energies can also be rejected. The remaining possibility is the one shown in Figure 22j. This seems to be the most plausible scheme since it suggests levels with energies of 588.34, 856.94 and 876.44 keV, the gamma rays of which have all been observed.

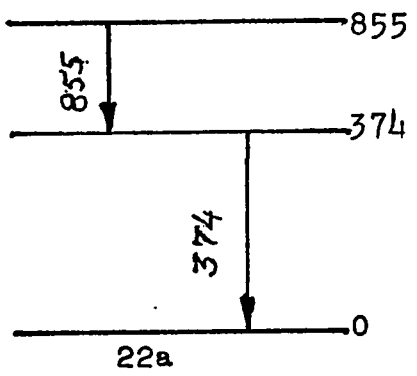

22a

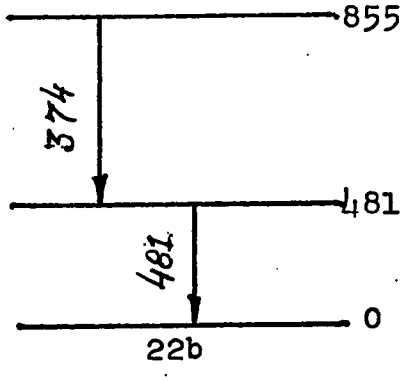

22b

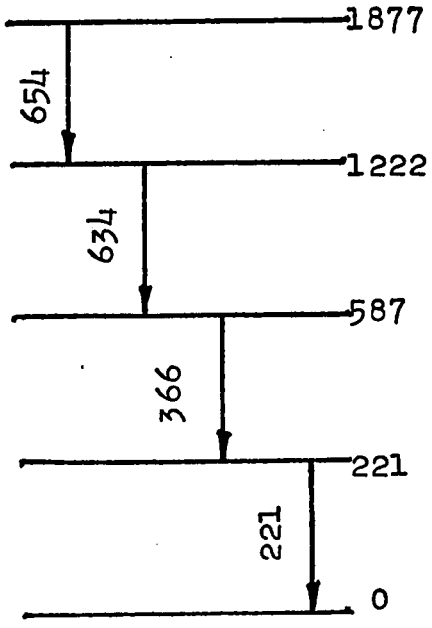

22c

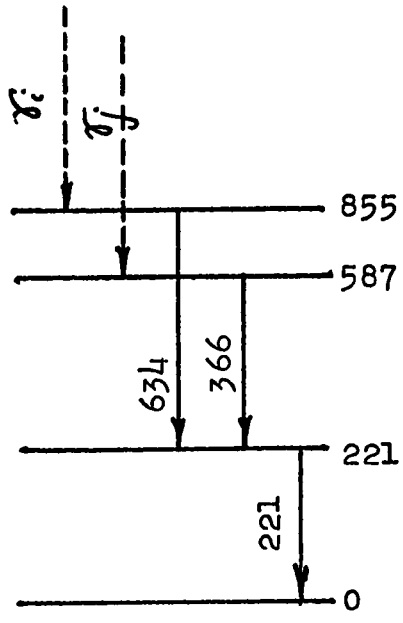

22d

(All energies in keV)

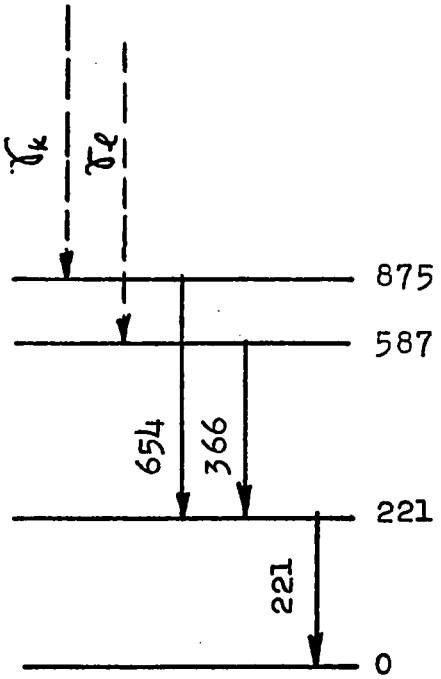

22e

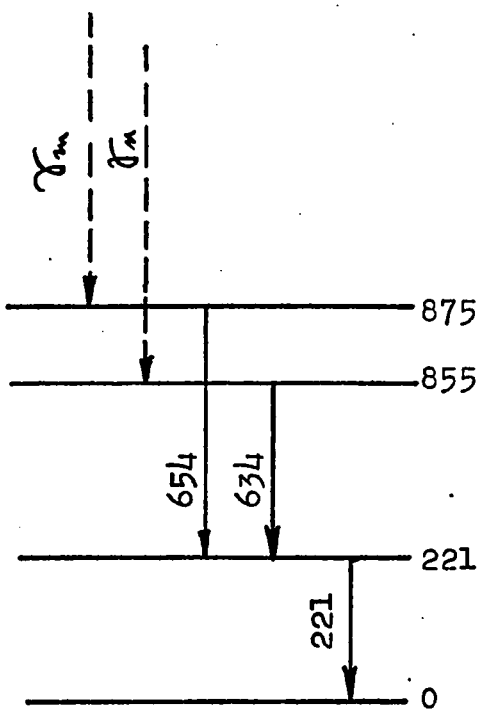

22f

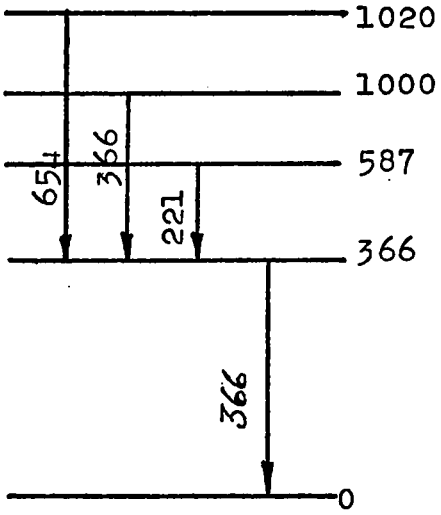

22g

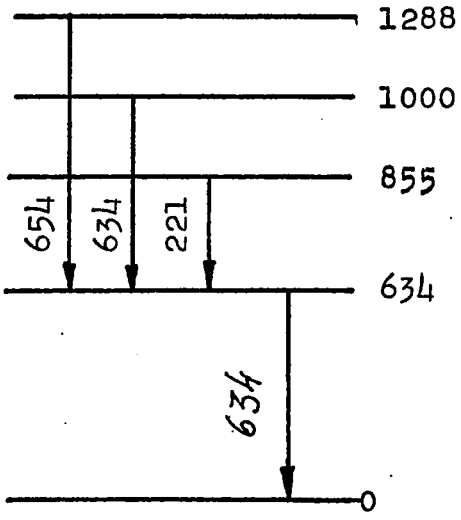

22h

(All energies in keV)

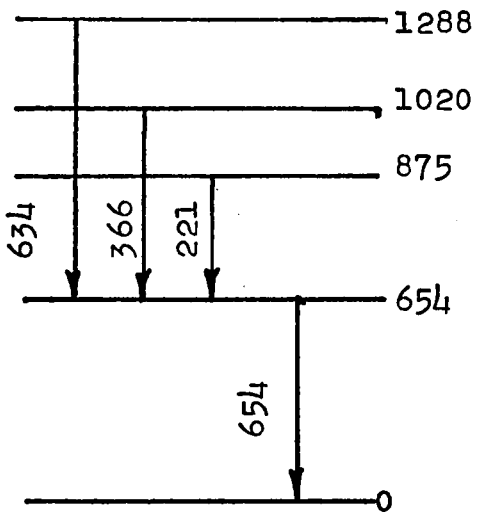

22i

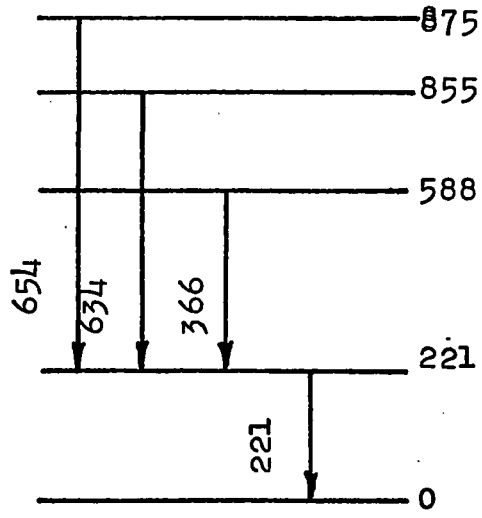

22j

(All energies in keV)

It has been mentioned in section 4.1 that the intensities of the gamma rays should also be consistent with the decay scheme proposed. Since in the course of these investigations, electron capture measurements could not be performed due to the unavailability of the necessary equipment one could not use this requirement to substantiate the proposed decay scheme. Relative intensities of the gamma rays were obtained through the use of the photopeak efficiency curve of the Ge(Li) detector, shown in Figure 12. These results are displayed in Table 8. Relative intensity obtained from the most prominent 481 keV gamma ray.

TABLE 9

Energy (keV)	Absolute Efficiency x 10^{-4}	Absolute Intensity	Relative Intensity % ($\pm$ 2%)
221	7.25	2.33	54
269	7.18	6.58	153
366	6.95	1.00	23
374	6.92	0.92	21
481	6.66	4.28	100
588	6.38	0.69	16
634	6.25	0.48	11
654	6.18	0.72	16
856	5.53	0.43	10
875	5.49	0.52	12

4.4 Discussion of results and Conclusion.

Having obtained the probable decay scheme of La^{135} on the basis of results obtained from singles spectra and coincidence measurements, it remains to give the spin and parity assignments to each level of the decay scheme. Since further measurements were not possible due

to the limited amount of required equipment, one can but present a discussion based on results obtained by previous investigators.

The spin and parity of the ground state of Ba^{135}, from measurements of magnetic moment performed by H.E. Walachi[9], are 3/2 . The ground state of La^{135}, as found by A.C.G. Mitchel[10] is 5/2 with a value of 5.6 for the log ft for the transition to the ground state of Ba^{135}. S. Morinbu et al[2] have found the following log ft values for the electron capture branches: 9.4, 6.7, 7.5, 7.3, and 7.0, these being for the transitions to the 221 keV, 481 keV, 588 keV, 856 keV and 875 keV levels respectively.

The 221 keV transition to the ground state is $M1(90\%)+E2$. This suggests the spin and parity of $1/2^+$, $3/2^+$, or $5/2^+$ for this level. The log ft value of this transition to this level is larger than 9.4, which implies that the transition is not allowed. The possibility of $3/2^+$ or $5/2^+$ is thus excluded. The assignment of $1/2^+$ for this level is in agreement with the one suggested by L.W. Fagg[11] following the results of a Coulomb excitation experiments.

The 481 keV level has an $M1+E2$ character so the transition to the $3/2^+$ ground state suggests the spin and parity of this level to be $1/2^+$, $3/2^+$ or $5/2^+$. Since the log ft value to this level is 6.7 then one can exclude the possibility of $1/2^+$. Grench et al[3] have observed a 265 keV transition corresponding to that between the 481 keV and the $1/2^+$ 221 keV level. However, this was not observed in this work nor was it reported by S. Morinbu et al[2] and so the 481 keV level is assigned to be $5/2^+$.

The multipolarity of the transition from the 588 keV level to the ground state and the presence of the 366 keV gamma ray transition to the $1/2^+$ 221 keV level leads to the assignment of $1/2^+$, $3/2^+$ or $5/2^+$ to this level. The log ft value to this level is 7.5 so the assignment of $1/2^+$ can be excluded.

The 856 keV level has a log ft value of 7.3 also there is the 634 keV gamma ray transition to the $1/2^+$ 221 keV state, the character of which was found to be M1+E2, by S. Morinbu et al[2] hence the spin and parity could either be $3/2^+$ or $5/2^+$.

The 875 keV level has a log ft value of 7.0 and there is also a transition to the $1/2^+$ 221 keV level via the 654 keV gamma ray, this then excludes any possibility for the assignment of $1/2^+$ to this level. The choice between the two remaining possibilities, the $3/2^+$ and $5/2^+$ spins and parities cannot be made in an affirmative manner. The fact that the 875 keV gamma ray was not observed in the X-Ray-gamma coincidence spectrum does not give any hint as to the choice to be made. Had the coincidence spectrum been allowed to accumulate for a much longer time then the 875 keV energy peak would probably have appeared. In order to make a more definite determination of the spins and parities, an internal conversion spectrum would be required. S. Morinbu et al[2] have made such measurements and have obtained a very low intensity peak for the 875 keV energy. Hence, based on their results, the choice of $3/2^+$ for this level is a more suitable one.

Although no new gamma transition energies or levels have been found in the course of these investigations, improvements have been achieved in the assigned energy values of the gamma rays. This can best

be seen when comparing results obtained by Grench[3] and S. Morinbu et al[2]..The comparison is shown in Table 10.

TABLE 10

Comparison of results for the gamma rays from La^{135}.

Grench	Morinbu	Author
	All energies in keV	
108 ± 4	103	-
218 ± 2	218	221 ± 0.5
256 ± 8	-	-
367 ± 3	367	366 "
375 ± 3	373	374 ± 1.0
481 ± 3	481	481 ± 0.5
587 ± 6	588	588 "
640 ± 12	633	634 "
-	655	654 "
865 ± 8	852	856 "
-	871	875 ± 1.0

The Author's results appear to be, in most cases, in fairly close agreement with those obtained by S. Morinbu et al[2]. From their experiments, however, they could not resolve the 367 - 373 keV, 633 -655 keV and 852 -871 keV gamma rays. They were able, however, to assign these energy values on the basis of their internal conversion experiments. The essential difference with the Author's results as compared to those of S. Morinbu et al[2] is that the 103 keV gamma ray has not been reported. Although a 94.35 keV (±0.5) gamma ray was observed, it did not fit the decay scheme, also the half life value obtained for it was not consistent with the remaining gamma rays, it is then excluded from the decay scheme.

The reliability of the results obtained here are based on the consistent manner in which they fit the decay scheme, this is shown in Figure 23.

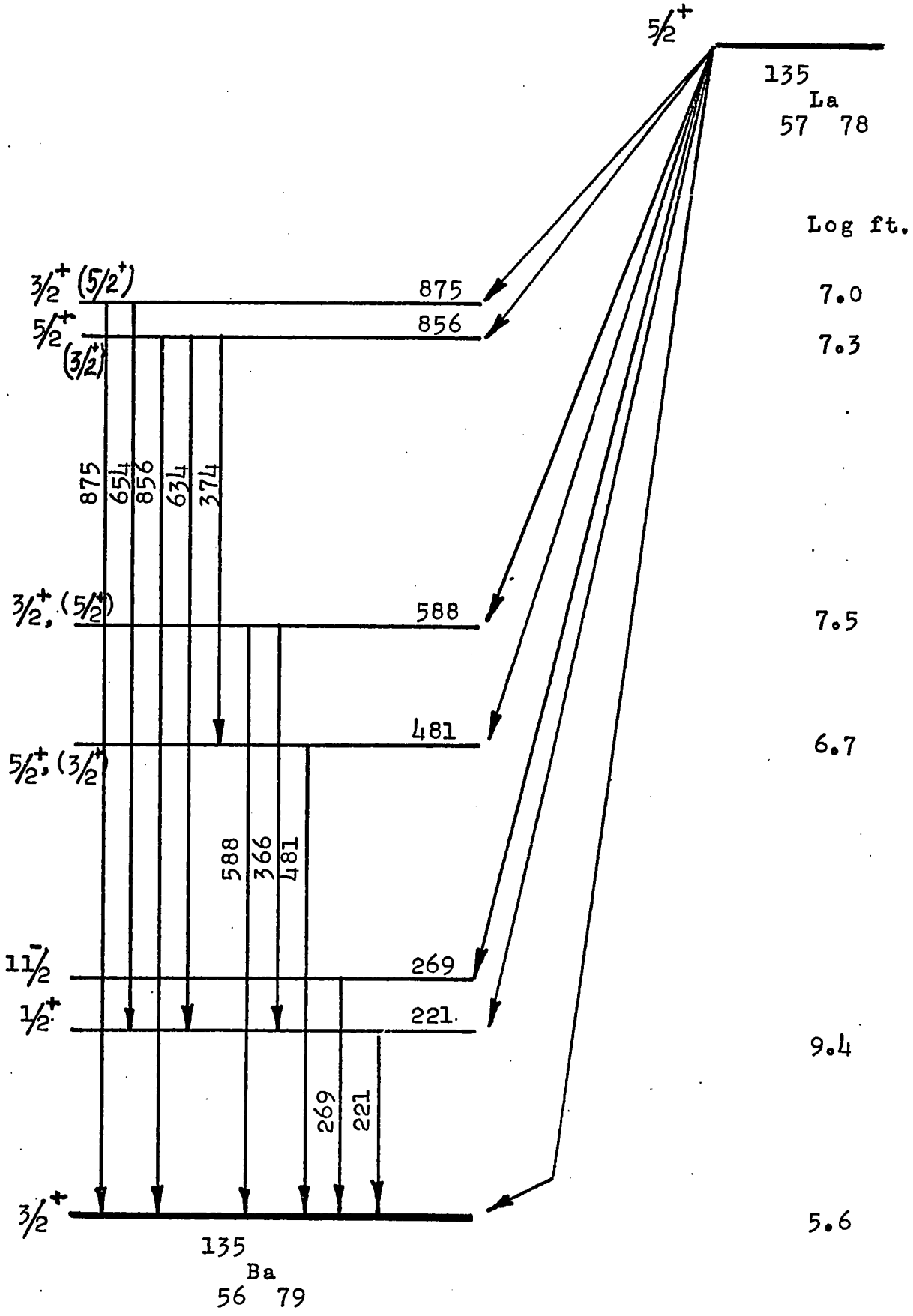

Figure 23. Proposed decay scheme.

(All energies in keV)

REFERENCE

1) K.E. Weimer, M.L. Pool and J.D. Kurbatov, Phys. Rev, 63 (1943), 67

2) S. Morinbu, T. Hirose and K. Hisatake, Nuclear Physics, 61 (1965), 613 (1965)

3) H.A. Grench and S.B. Burson, Phys. Rev, 137 (1965), B483

4) A. Goulding, Nucl. Instr. Meth, 43 (1966)

5) Siegbahn, Kai, Alpha-Beta-and Gamma-Ray Spectroscopy. Volume 1, 1965.
(North-Holland Publishing Company Amsterdam)

6) A. Melissinos, Experiments in Modern Physics; New York: Academic Press, 1967.

7) J.M. Blatt and V.F. Weisskopf, Theoretical Nuclear Physics; New York: John Wiley & Sons.

8) E. Fermi, Nuclear Physics; The University of Chicago Press, 1967.

9) H.E. Walchli and T.J. Rowland, Phys. Rev, 102 (1956), 1334

10) A.C.G. Mitchel, C.B. Creager and C.W. Kocher, Phys. Rev, 3 (1958), 1343

11) L.W. Fagg, Phys. Rev, 109 (1958), 100